ABSTRACT

The Effects of D-Amino Acids on *Staphylococcus Aureus* SA113 Biofilm Formation

Elizabeth R. Luper

Director: Sung Joon Kim, Ph.D.

Biofilms play a major role in the development of drug-resistant, persistent bacterial infections. D-amino acids have been proposed as biofilm inhibitors that prevent biofilm formation by incorporating into the peptidoglycan. We investigated this mechanism of inhibition using SA113, a *Staphylococcus aureus* clinical isolate that exhibits strong biofilm formation. The dispersive and inhibitory effects of D-tyrosine, D-phenylalanine, and D-proline were measured with a crystal violet biofilm assay. The addition of D-amino acids during or after biofilm formation did not disperse the biofilm or inhibit its formation. To study the proposed D-amino acid incorporation into peptidoglycan, SA113 cells were treated with mutanolysin and then analyzed with liquid chromatography-mass spectrometry (LC-MS). Our initial LC-MS analysis of SA113 grown in the presence and absence of D-amino acids suggested that peptidoglycan composition was not affected by the addition of D-amino acids.

APPROVED BY DIRECTOR OF HONORS THESIS:

_____

Dr. Sung Joon Kim, Department of Chemistry & Biochemistry

APPROVED BY THE HONORS PROGRAM:

_____

Dr. Andrew Wisely, Director

DATE: _____

THE EFFECTS OF D-AMINO ACIDS ON *STAPHYLOCOCCCUS AUREUS* SA113 BIOFILM FORMATION

A Thesis Submitted to the Faculty of

Baylor University

In Partial Fulfillment of the Requirements for the

Honors Program

By

Elizabeth R. Luper

Waco, Texas

May 2014

TABLE OF CONTENTS

ACKNOWLEDGMENTS

I would like to express my gratitude to Dr. Sung-Joon Kim, my Baylor faculty advisor, for mentoring while I was working on my undergraduate honors thesis. I appreciate the opportunity he gave me to work in his laboratory and the guidance he provided throughout the research and writing process. I would also like to thank James Chang, Ph.D. student, for his commitment to mentor me during my research. His constructive criticism of my ideas and writing provided me with invaluable insight. I would not have been able to accomplish the thesis without their guidance.

CHAPTER ONE

Introduction

Staphylococcus aureus *Biofilm*

Biofilm is a community of cells embedded within an extracellular matrix that forms a protective structure. The matrix is mostly composed of polysaccharides, polysaccharide intercellular antigen, staphylococcal and host proteins, extracellular DNA, and teichoic acids, which are phosphate rich anionic glycopolymers (Archer et al., 2011 and Swoboda et al., 2009). This matrix helps sessile communities of differentiated and organized bacteria to live and attach to inert or living surfaces (Figure 1).

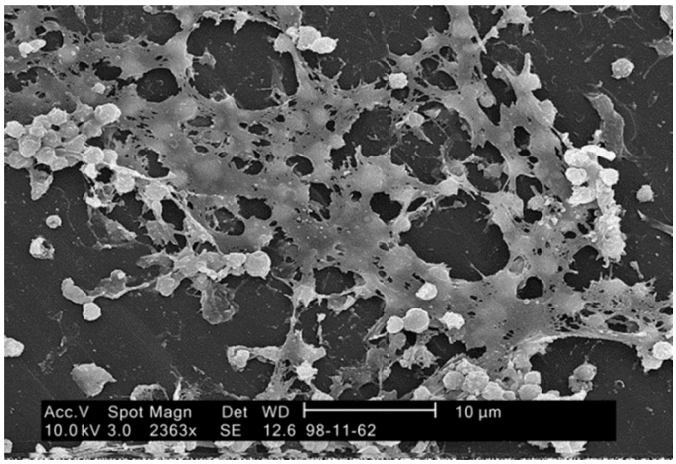

Figure 1. Electron micrograph of *S. aureus* found on the surface of an indwelling catheter. The biofilm forms a web-like structure between the cocci. (Donlan M. R., 2001).

S. aureus biofilm presents a major medical problem because it protects *S. aureus* cells from antimicrobial agents and host immune responses (Otto, 2008, Chuard et al., 1991). *In vitro* studies demonstrate that the effective bactericidal concentration of

antibiotics against bacteria in a biofilm must be 100 to 1,000 times greater than that needed to eliminate bacteria in planktonic stages (Ceri et al., 1999). Research of methods to facilitate the elimination of *S. aureus* is of interest to the medical community because of the infections caused by the bacteria.

S. aureus is a gram-positive coccus bacterium, found on skin and mucous surfaces. The bacteria can cause potentially deadly infections. Multi-drug resistant *S. aureus* is of great clinical relevance due to its prevalence in hospital environments, especially on indwelling medical devices (Archer et al., 2011). Methicillin-resistant *S. aureus* (MRSA) and vancomycin-resistant *S. aureus* (VRSA) strains are antibiotic resistant threats. According to the Centers for Disease Control and Prevention (CDC) 2013 report, 80,461 invasive MRSA infections and 11,285 related deaths occurred in 2011. Also, "an unknown but much higher number of less severe infections occurred in both the community and in healthcare settings" (CDC, 2013). The CDC has acknowledged 13 cases of VRSA in the United States since 2002, and stated the bacteria to be of concern, "leaving few or no treatment options" (2013). The use of indwelling medical devices increases the risk of *S. aureus* infections because they provide an ideal site for bacterial aggregation and biofilm formation (Herrmann et al., 1988).

Research about biofilm development and destruction can offer solutions to the growing problem of biofilm-related *S. aureus* infections. Biofilm-related diseases caused by *S. aureus* include osteomyelitis (the infection of bones), periodontitis (the infection and inflammation of the ligaments and bones around teeth), and peri-implantitis, which is the inflammation of tissue around dental implants (Archer et al., 2011). *S. aureus* biofilm is also at the source of 1) chronic wound infections, such as the inflammation disorder

chronic rhinosinusitis (Hamilos, 2013), 2) endocarditis, which is an infection of heart valves, 3) ocular infections, 4) polymicrobial biofilm infections, 5) cystic fibrosis (Goerke and Wolz, 2010), and 6) infections associated with indwelling medical devices, such as urinary catheters and prosthetic heart valves, and orthopedic devices (Archer et al., 2011). Biofilms are commonly associated with indwelling medical devices because of their need for a surface on which to form. Biofilms can cause chronic infections by providing bacterial resistance to antimicrobial agents. Biofilms facilitate *S. aureus'* resistance to antimicrobial agents via two main mechanisms: "(1) prevention of the antibacterial substance from reaching its target, e.g. by limited diffusion or repulsion, and (2) the specific physiology of a biofilm, which limits the efficacy of antibiotics, mainly of those that target active cell processes and which may also include specific subpopulations of resistant cells ("persisters')" (Otto, 2008 and Keren et al., 2004).

Biofilm Inhibition by D-amino acids

One method suggested for disrupting pre-existing biofilm or preventing its growth is to introduce D-amino acids into the environment surrounding the biofilm. D-amino acids are the enantiomers of L-amino acids, the building blocks of proteins found in most living organisms. In January 2011, Harvard researchers led by Dr. Richard Losick of the Molecular and Cellular Biology department filed an application for a patent of the use of D-amino acids for "treating or reducing biofilms, treating a biofilm-related disorder, and preventing biofilm formation." Losick's research group published an article in 2010 about the ability of D-amino acids to disperse and inhibit biofilm growth in gram-positive *Bacillus subtilis*, *S. aureus* and gram-negative *Pseudomonas aeruginosa* strains (Kolodkin-Gal, I. et al., 2010). The *S. aureus* strain they examined was a lab isolated

strain. Further research supported the statement that D-amino acids can inhibit the growth of *S. aureus* biofilm (Hochbaum et al., 2011). Applications of this discovery might include medical devices and scaffolds for open fractures which slowly release D-amino acids (Hochbaum et al., 2011 and Sanchez et al., 2013).

D-amino acids were first suggested as potential biofilm inhibitors because of the discovery of their secretion in stationary phase cultures of *Vibrio cholerae* and *B. subtilis* (Lam et al., 2009). It is advantageous for bacteria to be able to switch between the planktonic and biofilm-associated forms, based on environmental cues (Karatan and Watnick, 2009). Biofilms can sequester nutrients from the environment for the bacterial cells, protect bacteria from antimicrobial agents, and allow the spread of biofilm-associated bacteria (Archer et al., 2011). However, changes in environmental conditions or in biofilm size, preventing some cells from accessing nutrients or avoiding toxic wastes, could lead to the necessity to return to the planktonic form (Karatan and Watnick, 2009). The planktonic mode describes single bacterial cells unfixed to a surface. Thus, biofilms must be able to trigger their own disassembly. Based on this conclusion, Kolodkin-Gal et al. looked at whether the media from old biofilms produced factors that would trigger biofilm disassembly (2010). After observing that factors in the media inhibited biofilm formation, the group proposed that D-amino acids, produced by cells in the stationary phase, represented a set of biofilm dispersing and inhibiting factors (Kolodkin-Gal et al., 2010).

The mechanisms of action of D-amino acid biofilm inhibition and dispersal are still unclear. Kolodkin-Gal et al. showed that D-amino acids are incorporated into the peptidoglycan cell wall of *B. subtilis* (Kolodkin-Gal et al., 2010). They hypothesized that

the D-amino acids replaced the terminal D-alanine in the peptidoglycan of *B. subtilis*, preventing TasA amyloid fibers (fibers of insoluble protein aggregates) from binding to the cell walls (Kolodkin-Gal et al., 2010). TasA, a major protein component of *B. subtilis* biofilms, helps form *B. subtilis*' biofilm extracellular matrix (Branda et al., 2006 and Romero et al., 2010). The Losick group demonstrated that D-amino acids prevent the adhesion of TasA to *B. subtilis* cell wall (Kolodkin-Gal et al., 2010). However, *S. aureus* and *P. aeruginosa* do not secrete biofilm matrix-associated amyloid fibers, suggesting that a universal mechanism of D-amino acid biofilm inhibition does not exist (Cava et al., 2010).

Hochbaum et al. proposed that D-amino acids inhibit biofilm formation in *S. aureus* by changing the properties of the extracellular matrix and thus preventing cellular aggregation (Hochbaum et al., 2011). In *S. aureus* biofilm formation, surface proteins play important roles of cellular adhesion in the extracellular matrix (Cucarella et al., 2001, Geoghegan et al., 2010, O'Neill et al., 2008 and Schroeder et al., 2009). Hochbaum et al. used fluorescence and confocal scanning laser microscopy to determine that D-amino acids inhibit the accumulation of surface proteins at the cell wall (Hochbaum et al., 2011). D-tyrosine, D-phenylalanine, and D-proline were shown to be the most effective at biofilm inhibition (Hochbaum et al., 2011). This inhibition of cell surface-associated protein accumulation resembles the inhibition of TasA binding to the cell wall in *B. subtilis*. D-amino acids were therefore hypothesized to prevent surface proteins from accumulating by incorporating into the peptidoglycan (Kolodkin-Gal et al., 2010 and Hochbaum et al., 2011).

The inhibition of *S. aureus* biofilm development by D-amino acids may be due to incorporation of these D-amino acids into peptidoglycan, resulting in structural changes of the cell wall. Kuru et al. have shown that fluorescent D-amino acids can be incorporated into peptidoglycan biosynthesis (2012). Peptidoglycan forms the majority of the cell wall of gram-positive bacteria and is found on the outside of the membrane. Thus, peptidoglycan may have a very important role in biofilm formation, since it is the surface of gram positive cells where external components can attach. Peptidoglycan is "a polymer composed of linear glycan strands made up of repeating disaccharide units of N-acetyl glucosamine (GlcNAc) and N-acetylmuramic acid (MurNAc) cross-linked by short peptides," which include certain D-amino acids such as D-alanine (Cava et al., 2010). In *S. aureus*, alternating β1-4-linked GlcNAc and MurNAc are cross-linked with peptide chains containing L-alanine, D-isoglutamine, L-lysine, and D-alanine residues, and an interpeptide pentaglycyl bridge (Figure 2) (Vollmer et al., 2008).

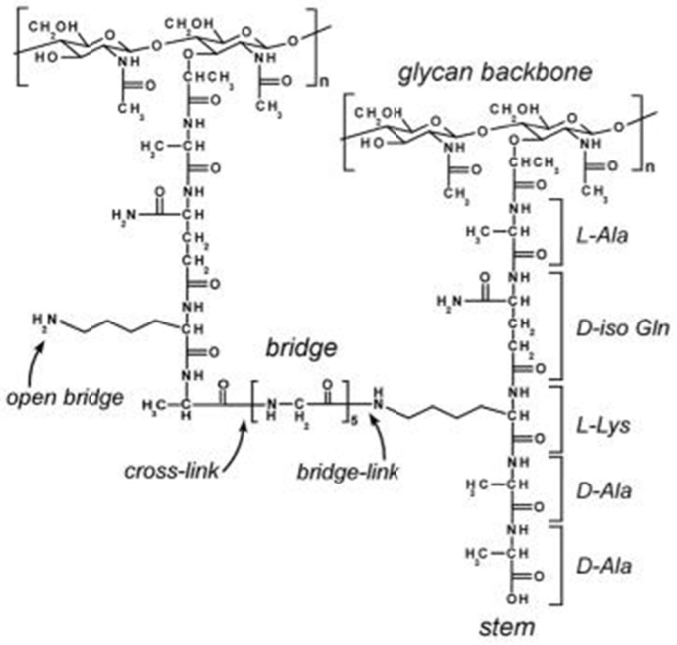

Figure 2. Structure of peptidoglycan (Kim, S. J. et al., 2013).

Hypothesis: S. aureus *Biofilm Inhibition by Incorporation of D-Amino Acids into Peptidoglycan*

We were interested in confirming that D-amino acids disperse pre-existing biofilm and inhibit the formation of biofilm of a clinical strain of *S. aureus*. We chose to use mainly SA113, which is a clinically-isolated, strong biofilm-producing strain. We used a crystal violet assay to quantify biofilm growth. Crystal violet was used to stain surface-attached cells of *S. aureus* that were grown in media with and without D-amino acids. The crystal violet biofilm assay was based on the protocol developed by O'Toole and Kolter which involves staining cells attached to a surface because of biofilm (Kolodkin-Gal et al., 2010 and O'Toole and Kolter, 1998).

We also were interested in confirming that D-amino acids can inhibit biofilm by being incorporated into the peptidoglycan. This specific question lies within a larger investigation about the role that peptidoglycan plays in biofilm development. We used liquid chromatography with mass spectrometry to analyze peptidoglycan fragments from *S. aureus* grown in the absence and presence of D-tyrosine. D-tyrosine was used because previous research showed it to be effective at inhibiting biofilm formation for concentrations as low as 50 μM (Kolodkin-Gal et al., 2010 and Hochbaum et al., 2011). Peptidoglycan fragmentation was produced by digesting the cell walls with mutanolysin, which cuts the β1-4 glycosidic linkages of the glycan backbone. A library of mass-to-charge ratios of possible peptidoglycan fragments with incorporated D-tyrosine was compared to the data obtained from mass spectrometry sample analysis. Matches would indicate the presence of D-tyrosine in the peptidoglycan. Thus, the presence or absence of D-tyrosine in peptidoglycan could be elucidated from mass spectrometry.

CHAPTER TWO

Materials and Methods

Growth Conditions

Before biofilm dispersion and inhibition experiments, SA113 (Dr. Berger-Bachi's lab at the Institute of Medical Microbiology, University of Zurich, Zurich, Switzerland) overnight cultures were prepared by inoculating TSB media (BD Bacto) with 1% SA113, and incubating it at 37 °C and 90 rpm, overnight.

For biofilm inhibition and dispersion experiments in glass test tubes, 30 μL of SA113 overnight culture was pipetted into 3 mL of TSB media with the appropriate additives of D-amino acids and glucose in each test tube. The following 5 conditions were used: 1) 1% glucose (Alfa Aesar) (48 hours), 2) 1% glucose and 100 μM D-tyrosine (Alfa Aesar) (48 hours), 3) 1% glucose added initially and 2.5 mM D-tyrosine added after 24 hours (total time was 48 hours), 4) no additives (48 hours), and 5) 2.5 mM D-tyrosine (24 hours). The test tubes were parafilmed and placed in the incubator at 37 °C and 180 rpm. These test tubes were used for liquid chromatography-mass spectrometry sample preparation.

For biofilm dispersion experiments in 24-well plates, 10 μL of SA113 overnight culture was grown in 1 mL of TSB media with 1% glucose in each well. Each plate was placed in an incubator at 37 °C or 37.5 °C and 90 rpm. After 24 hours, the dispersion plates were removed from the incubator and the media from each well was pipetted out. 1 mL of TSB media with the appropriate additives of 0.25 mM to 10 mM D-tyrosine, D-phenylalanine (Alfa Aesar), and D-proline (Pure Chemistry Scientific Inc.) and of

glucose were added to each well. The plates were returned to the incubator at 37 °C or 37.5 °C and 90 rpm. After 24 hours, the plates were removed from the incubator, photographed, and assayed for biofilm formatting, using the crystal violet asssay.

For biofilm inhibition experiments in 24-well plates, 10 µL of *S. aureus* strain SA113 or RN4220 overnight culture were pipetted into 1 mL of TSB media with the appropriate additives of D-amino acids (0.25 mM – 10 mM) and glucose (0% or 1%) in each well. Each plate was placed in an incubator at 37 °C or 37.5 °C and 90 rpm. After 24 hours, the plates were removed from the incubator, photographed, and assayed for biofilm formation using crystal violet.

Crystal Violet Assay

The biofilm grown in the wells of 24-well plates was stained with crystal violet (Alfa Aesar) according to the following procedure. The media from each well was removed by pipetting. Next, each well was washed twice with 1 mL each time of phosphate buffered saline (PBS) buffer, pH = 7.4. Then, 500 µL of 0.1 % crystal violet in deionized water were added to each well. The wells were incubated with crystal violet for 15 minutes. After removing the crystal violet by pipetting, each well was washed twice with 1 mL of deionized water. The water was removed, then the plates were dried at 50 °C for 6.5 hours. Then, 500 µL of 95 % ethanol were added to each well. After incubating for 2.5 hours at 30 °C and 180 rpm, the ethanol was collected in microcentrifuge tubes and stored at -80 °C for optical density analysis. Optical density analysis was performed on thawed samples, after 4 fold and 20 fold dilutions in deionized water. The absorbance at 595 nm was measured with a UV-Vis spectrophotometer.

Liquid Chromatography-Mass Spectrometry (LC-MS) Sample Preparation

Samples from the biofilm experiments in glass test tubes were prepared for LC-MS analysis. To collect the samples for LC-MS sample preparation, the media was removed by pipetting. The samples were washed twice with 1 mL each time of PBS buffer, pH = 7.4. They were each resuspended in 1 mL of PBS buffer in a microcentrifuge tube. The tubes were placed in boiling water for 10 min. They were then centrifuged for 2 minutes at 10,000 rpm. The supernatants were removed and the pellets were resuspended in 1 mL of 20 mM HPLC (high performance liquid chromatography) grade Tris buffer (pH = 8.0). After repeating the centrifugation process, the pellets were again resuspended in 1 mL amounts of HPLC-grade Tris buffer (pH = 8.0). Next, 50 μL of mutanolysin (Sigma-Aldrich) were added to each sample. The mutanolysin was from a bottle of 5000 units of freeze-dried enzyme that were dissolved in 600 μL of 20 mM Tris buffer. The solutions were vortexed and set aside for approximately 24 hours.

Filtration of the samples was a two-step process. First, the samples were filtered with a 0.45 μm filter. Next, the filtrates were filtered with a 30 kDa cutoff filter. Cation exchange was performed on the filtrates, using a cation exchange column and 20 mM HPLC-grade Tris buffer (pH = 8.0). The collected solutions were stored at -80 °C until mass spectrometry analysis could be performed.

Liquid Chromatography-Mass Spectrometry (LC-MS)

The samples analyzed with LC-MS were collected from the biofilm experiments in glass test tubes. LC-MS analysis of the samples was performed with the ACQUITY UPLC System (Waters) and the SYNAPT G2-Si High Definition Mass Spectrometer

(Waters). The mass spectrometer was set to run TOF-LC/MS (time of flight-liquid chromatography/mass spectrometry). The instrument was set on the positive mode. The gradient program on the instrument was the following. Initially, 99% of the mixture was water + formic acid, and 1% was acetonitrile + methanol. After 30 minutes, 50% of the mixture was water + formic acid, and 50% was acetonitrile + methanol. At 31 minutes, the solvent mixture was 15% water + formic acid and 85% acetonitrile + methanol. At 37 minutes, the solvent mixture was returned to the initial ratio of 99:1. The flow rate was 0.45 μl/min.

Data Processing

Data from the LC-MS sample analysis was processed with the Waters MassLynx Mass Spectrometry Software. A library of masses was used to analyze the data. The library was generated by drawing potential structures with ChemBioDraw, a software system from CambridgeSoft.

CHAPTER THREE

Results

Biofilm Production

First attempts at growing biofilm-producing *S. aureus* consisted in looking for biofilm growth in glass test tubes. Biofilm was expected to be a thin white layer or film that stuck to the sides or bottom of the tubes. SA113, a clinically-isolated strain which produces large amounts of biofilm, was grown overnight in various conditions. White pellets were then visible at the bottom of all the tubes, except the tube without glucose (Figure 3). The pellets of cell aggregates corresponded to biofilm growth. These samples were collected for mass spectrometry analysis.

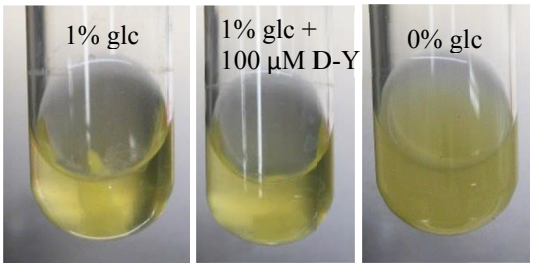

Figure 3. Photograph of overnight cultures of SA113 grown in TSB with additives. The additives are, from left to right: 1% glucose, 1% glucose + 100 µM D-tyrosine, and no additives. *S. aureus* biofilm is visible as a pellet at the bottom of each test tube for all of the conditions, except the tube without glucose (far right).

The subsequent experiments were set up in 24-well plates. Difficulty had arisen when trying to decant and rinse the biofilm in the glass test tubes without loss of biofilm. Also, the biofilm did not seem to "stick" to the glassware. The glass tubes were rather cumbersome and did not allow for as many experimental designs. While having glass

tubes provided large sample amounts for use in mass spectrometry, the large sample size was not necessary for the purposes of observing differences in biofilm formation based on the presence of D-amino acids. Thus, 24-well plates were used instead of glass tubes.

When growing SA113 in 1 mL wells in 24 well-plates, the yellow media became cloudy and, in the presence of glucose, a thin, opaque, white, filmy substance formed on the bottom of each well. This substance was partially attached to the bottom and side walls of the well. Sometimes it had a net-like characteristic to it, and seemed thicker in the center of the well. Sometimes the substance was more of a uniform, cracked film over the bottom of the well. Figure 4 is a photograph of one of the plates before media removal. The substance was assumed to correspond to SA113 biofilm. As far as durability, the majority of the biofilm stayed in the wells after removing the media with a micropipette, and rinsing the biofilm with PBS buffer twice. However, some chunks or flakes of biofilm were sometimes aspirated into the micropipette tip if the media and wash were removed too quickly. Thus, the experimenter had to exercise delicacy, uniformity, and patience while washing the biofilm.

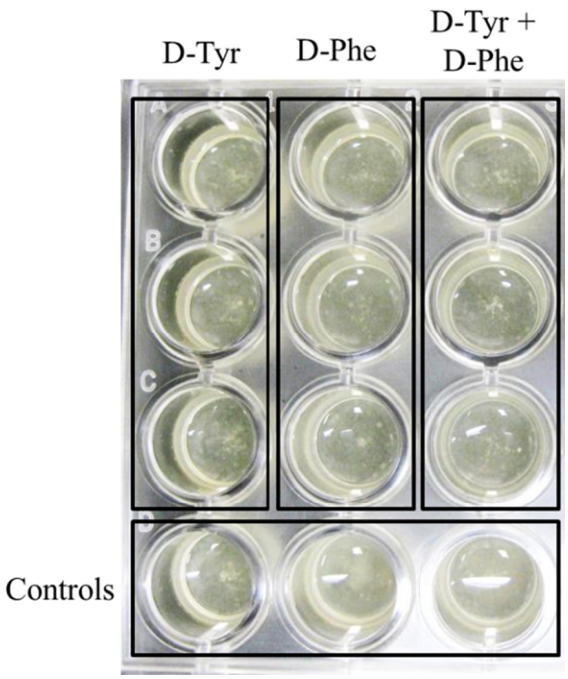

Figure 4. Photograph of a D-amino acid dispersal experiment plate before media removal. Each well contained SA113 and TSB and 1% glucose, except well D2, which had the SA113 ΔccpA strain. After 24 hours of growth without D-amino acids, the media was exchanged for media with D-amino acids, to test for dispersal of biofilm. A1-C1 included D-tyrosine, at 2.5 mM, 1 mM and 0.25 mM, respectively. A2-C2 included D-phenylalanine, at 2.5 mM, 1 mM and 0.25 mM, respectively. A3-C3 included an equimolar combination of D-tyrosine and D-phenylalanine, at 1.25, 0.5 and 0.125 mM each. D1-3 had no D-amino acids. For D3 there was no media change.

Our results indicated that SA113 required glucose to form biofilm. Figure 3 shows that SA113 grown in TSB media without glucose did not produce biofilm, but rather stayed in the planktonic phase. This is evidenced by the lack of cell aggregation and the cloudiness of the sample. We recorded additional observations that SA113 did not form biofilm in test tubes without glucose, including whether or not 2.5 mM D-tyrosine was added. In 24-well plate experiments, SA113 formed less to no biofilm in wells without glucose, as illustrated in Figure 5 and recorded in our lab notebook.

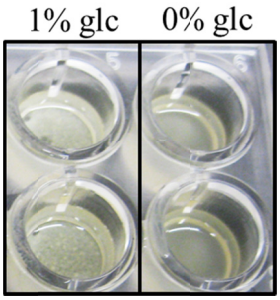

Figure 5. Photograph of SA113 biofilm growth in wells with TSB and 1% or no glucose.

Crystal violet staining was used to quantify changes in biofilm growth. After trying out 0.1%, 0.01% and 0.001% crystal violet solutions, the 0.1% solution seemed to provide the best staining concentration. The 0.1% solution stained all of the biofilm a bright purple color. The inside edges of the wells tended to be the most stained. This observation might be explained by the edges providing an ideal place for biofilm growth because of the available scaffolding, or by the crystal violet solution collecting along the edge. 95% ethanol was used to collect the dye, and the optical densities were measured after 4 fold dilutions. The dilutions were necessary because of the high absorbance of ethanol with concentrated concentrations of crystal violet, but the 0.1% solution was still used to stain in order to make visualization easier.

Biofilm Dispersion

Attempts at dispersing biofilm with D-tyrosine, D-phenylalanine, and/or D-proline were unsuccessful. Observations from the test tube dispersal experiments included the following. Biofilm was observed 24 hours after addition of 2.5 mM D-tyrosine to a pre-formed biofilm. Biofilms were also observed 24 hours after media exchanges with 1% glucose and the conditions of 2.5 mM D-tyrosine, 10 mM D-phenylalanine, and 2.5 mM D-tyrosine with 5 mM D-phenylalanine.

Visual observation of biofilm presence in 24-well plates before and after crystal violet staining showed a lack of significant effect of these D-amino acids on the presence or amount of biofilm. Figures 4, 6, and 7 illustrate the visual similarity of many wells of SA113 grown in various D-amino acid dispersal conditions. The initial observations of the various plates were inconclusive.

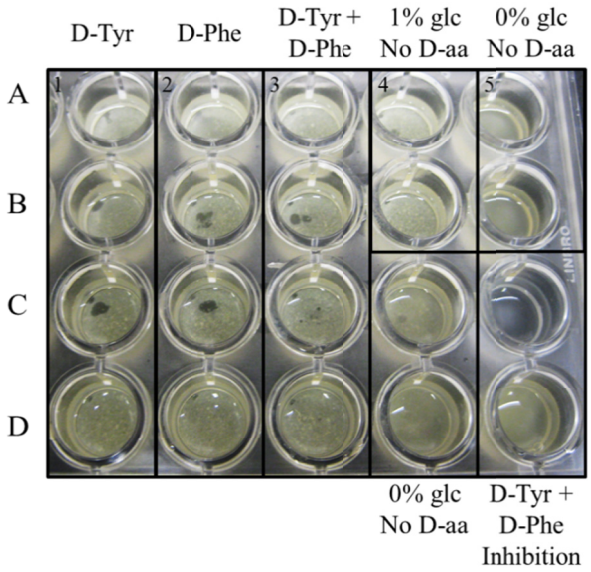

Figure 6. Photograph of a SA113 D-amino acids dispersion experiment, before media removal for crystal violet straining. SA113 was grown in TSB with 1% glucose in wells in columns 1-4. In column 6, SA113 was grown in TSB without glucose. After 24 hours, the media was exchanged with TSB with the following additives. In column 1, wells A-D corresponded to 2.5 mM, 2.5 mM, 1 mM, and 0.5 mM D-tyrosine, respectively. Column 2 consisted of wells A-D with 10 mM, 5 mM, 1mM, and 0.5 mM D-phenylalanine, respectively. Column 3 consisted of wells A-D with 2.5 mM D-tyrosine + 5 mM D-phenylalanine, 2.5 mM 1:1 ratio, 0.5 mM 1:1 ratio, and 0.25 mM 1:1 ratio of D-tyrosine and D-phenylalanine, respectively. In column 4 and wells A5 and B5, no D-amino acids were added, and 1% or 0% glucose was added. Wells C5 and D5 were inhibition tests.

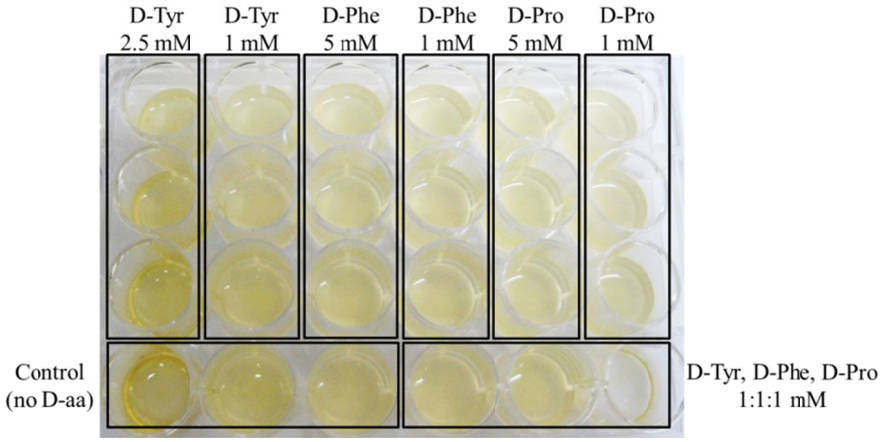

Figure 7. Photograph of a SA113 D-amino acids dispersion experiment, before media removal for crystal violet staining. SA113 strain was grown in TSB with 1% glucose. After 24 hours, the media was exchanged with TSB with 1% glucose and additives, as described on the figure.

With crystal violet staining, the lack of biofilm dispersion due to D-amino acids became more evident. Figures 8, 9, and 10 provide images for various crystal violet assays of the dispersal effects of D-tyrosine, D-phenylalanine, D-proline and various combinations of the three D-amino acids on SA113 biofilm. These figures illustrate the large presence of biofilm in each well. In some cases, wells with D-amino acid solutions seemed to produce just as much, if not more, biofilm than the positive controls.

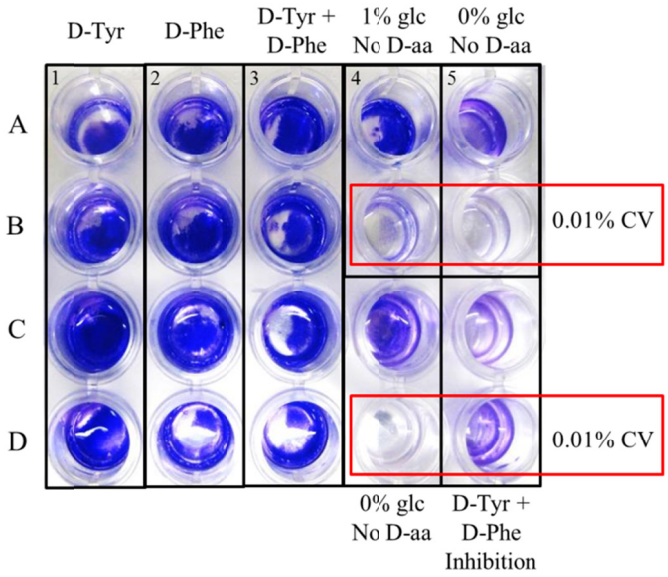

Figure 8. Photograph of the crystal violet assay of the SA113 D-amino acids dispersion experiment from Figure 6. 0.1% crystal violet was used for all wells, except wells B4-5 and D4-5, for which 0.01% crystal violet was used.

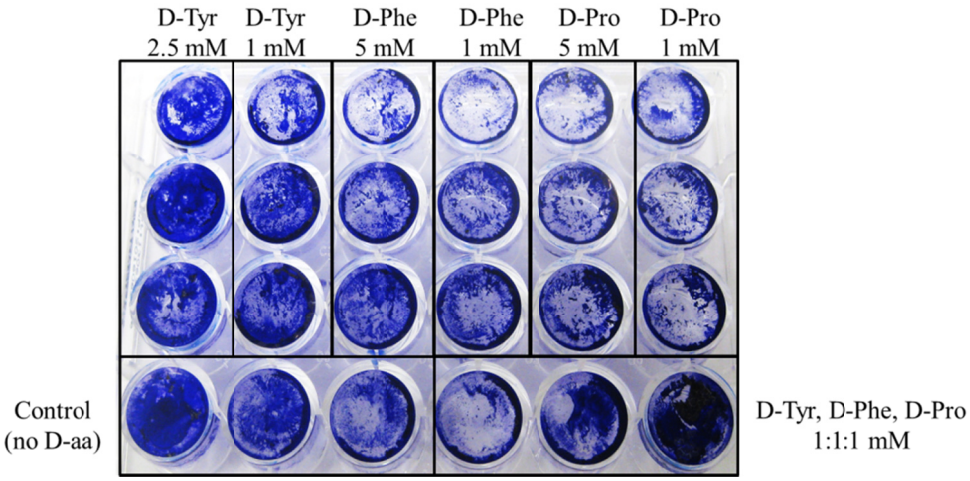

Figure 9. Photograph of the crystal violet assay of the SA113 D-amino acids dispersion experiment from Figure 7. SA113 was grown for 24 hours in TSB media containing 1% glucose, and then the media was exchanged with TSB with 1% glucose and additives, as described on the figure.

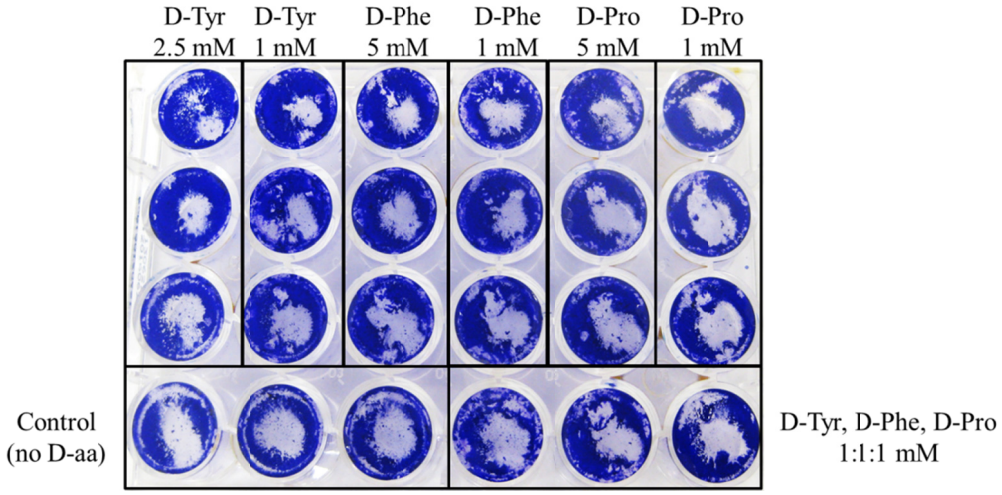

Figure 10. Photograph of the crystal violet assay of a SA113 D-amino acids dispersion experiment. SA113 was grown for 24 hours in TSB with 1% glucose, and then the media was exchanged with TSB with 1% glucose and additives, as described on the figure.

The optical density measurements showed similar results to the visual observations. The optical densities at 595 nm of the diluted ethanol collected from the crystal violet-assayed wells from D-amino acid biofilm dispersal tests showed a range of values which did not exhibit any major difference from the control. Figures 11, 12, and 13 display the optical densities with respect to the concentrations of D-amino acids present in the media used to replace the initial media containing 1% glucose to form pre-existing biofilm. According to Figure 11, the only biofilm sample which had an optical density below the error bar of the control, was from the 2.5 + 2.5 mM D-tyrosine and D-phenylalanine condition. Figure 11 provides a precursory evaluation of the effects of D-amino acids on SA113 biofilm because each condition was tested only once. Nevertheless, the results from Figure 11 suggest that neither D-tyrosine nor D-phenylalanine disperse pre-existing SA113 biofilm.

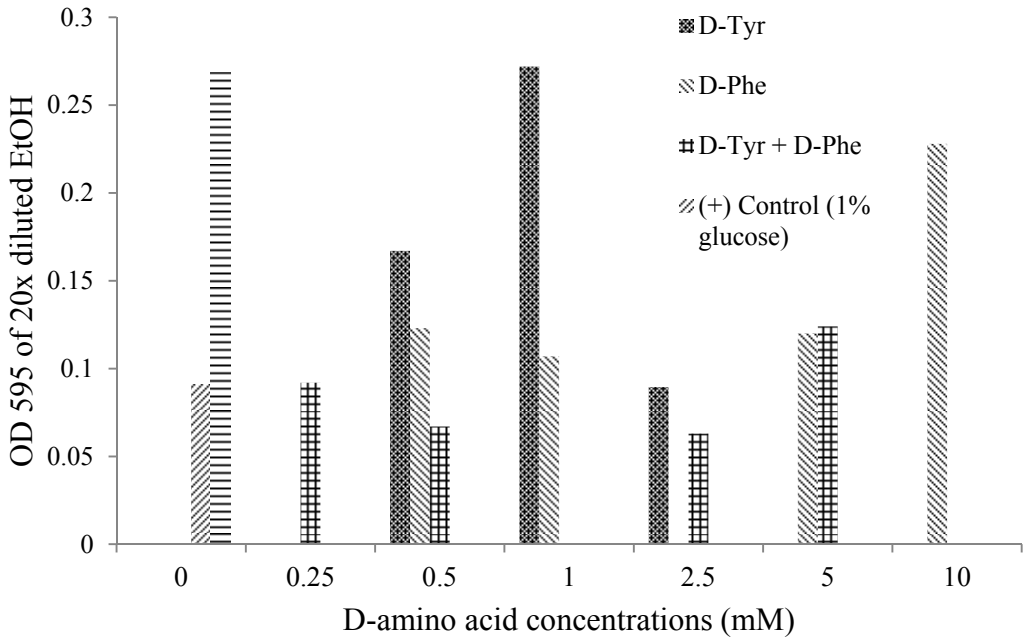

Figure 11. Chart representing the optical densities of diluted ethanol from the crystal violet assay from the D-amino acid biofilm dispersal experiment in Figures 6 and 8. The difference in crystal violet concentration was corrected for by multiplying by 10 the absorbance of ethanol from wells assayed with 10-fold diluted crystal violet.

Figures 12 and 13 show that 5 mM to 1 mM D-tyrosine, D-phenylalanine, and D-proline did not disperse pre-existing biofilm. In Figure 12, the error bar from the control overlaps with all of the average values of optical density measurements from various conditions. The control was SA113 biofilm formed in TSB media containing 1% glucose and no D-amino acids. The error bars are unfortunately rather large, which may be due to errors in the crystal violet analysis or inherent dissimilarities between biofilms. In Figure 13, all of the average optical densities are larger than the control, except for the combination of 1 + 1 + 1 mM D-tyrosine, D-phenylalanine, and D-proline. The error bar of the latter condition overlaps with the error bar of the control. Thus, Figure 13 also demonstrates that 5 mM to 1 mM D-tyrosine, D-phenylalanine, and D-proline did not provide any appreciable reduction to pre-existing biofilm.

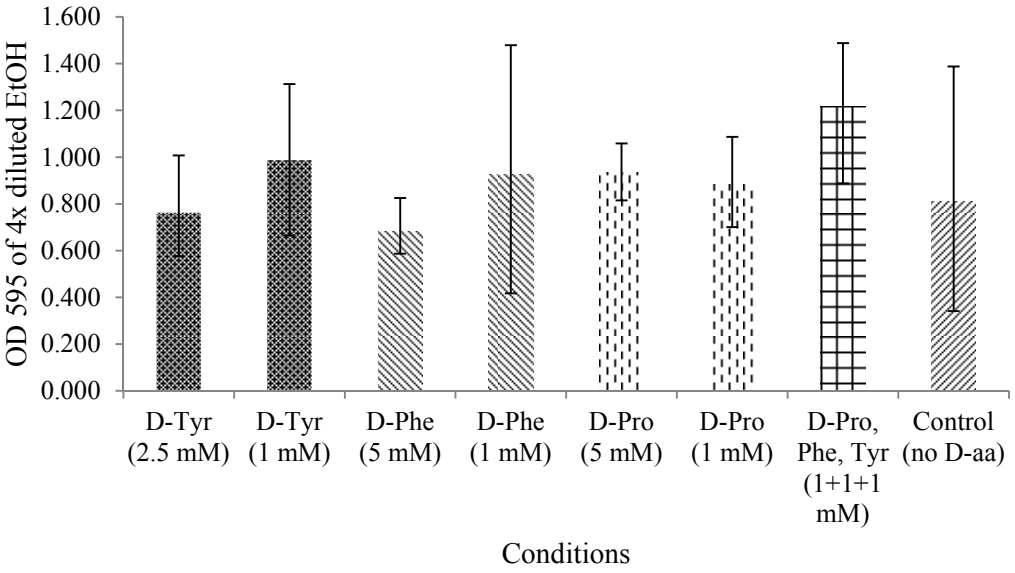

Figure 12. Chart representing the optical densities of diluted ethanol from the D-amino acid biofilm dispersal experiment in Figures 8 and 9. The error bars are based on the average sample standard deviation.

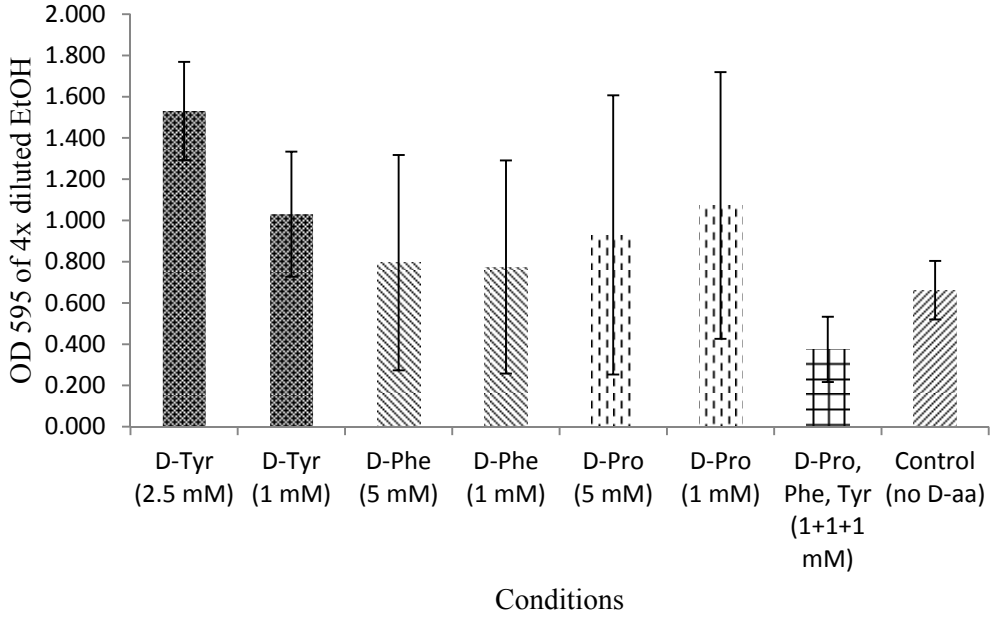

Figure 13. Chart representing the optical densities of diluted ethanol from the D-amino acid biofilm dispersal experiment in Figure 10. The error bars are based on the average sample standard deviation.

Biofilm Inhibition

The potential therapeutic benefits and the desire to better understand how biofilm, peptidoglycan, and extracellular components interact motivated the investigation concerning the mechanisms by which D-amino acids inhibit biofilm formation. Inhibition tests in glass test tubes suggested that D-amino acids may not inhibit biofilm formation. The second image in Figure 6 displays a test tube with a cell aggregate at the bottom, illustrating that TSB media containing 1% glucose and 100 μM D-tyrosine did not inhibit SA113 biofilm formation.

Upon visual inspection, Figures 14 does not show any marked difference between wells with and without D-amino acids. Figure 14 shows an increase in crystal violet coloring on the left-hand column. This may be due to uneven drying in the incubator. Figure 14 shows that large amounts of biofilm were nevertheless present when D-amino acids were initially present to inhibit biofilm formation. Figure 15 provides the average optical density measurements at 595 nm for the various conditions in Figure 14. According to Figure 15, the error bar of the control overlaps with all of the error bars of the other conditions, which range from 1 mM to 10 μM of D-tyrosine, D-phenylalane, D-proline, and an equimolar 10 μM combination of those three amino acids. Thus, none of the tested conditions provided statistically significant inhibition of biofilm formation, compared with the positive control.

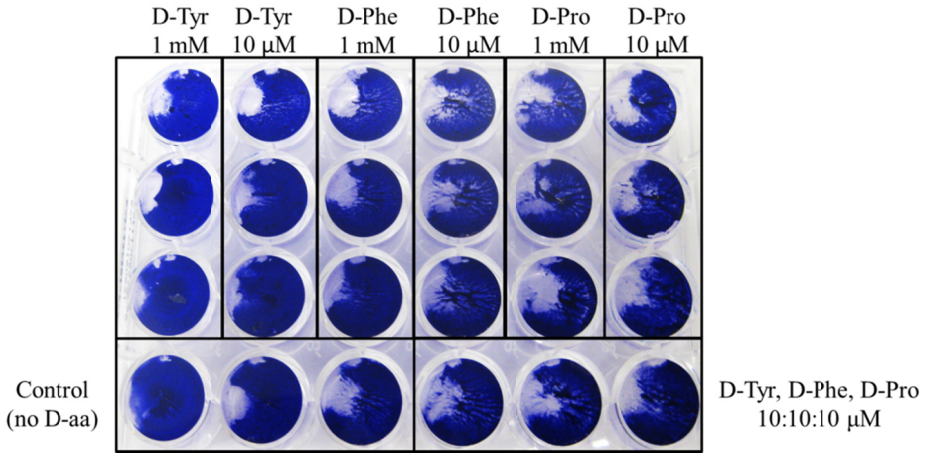

Figure 14. Photograph of the crystal violet assay of a SA113 D-amino acid biofilm inhibition experiment. SA113 was grown for 24 hours in TSB containing 1% glucose and additives, as listed in the figure.

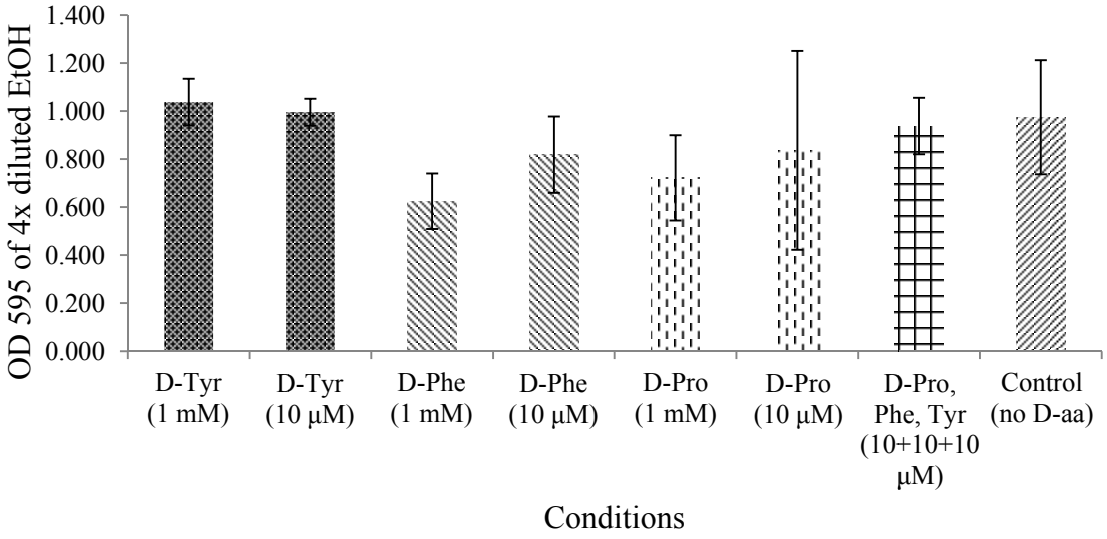

Figure 19. Chart representing the optical densities of diluted ethanol from the D-amino acid biofilm inhibition experiment in Figure 14. The error bars are based on the average sample standard deviation.

Because SA113 is a very strong biofilm former, we decided to test for D-amino acid inhibition of biofilm from a different *S. aureus* strain. We chose to run some similar tests with RN4220, which is a commonly used lab strain, used often in studying

virulence, resistance, and metabolics. D-amino acid inhibition tests on RN4220 biofilms also provided negative results. Figure 16 displays the presence of biofilm in wells grown in 1% glucose and the absence of biofilm in wells grown without D-amino acids. The biofilm is visible as a more opaque coloration at the bottom of the well. RN4220 that was grown without glucose remained in the planktonic phase, as seen by the differentiation in color and lack of cell aggregation at the bottom of the well (second column of Figure 16). Figures 17 and 18 provide the average optical densities at 595 nm of diluted ethanol. This ethanol was collected from crystal violet assays of 6 replicates of various conditions of media containing glucose and D-amino acids. The invariance of results in Figures 17 and 18 indicates that 50 to 500 μM concentrations of D-tyrosine, D-phenylalanine, and D-proline do not inhibit RN4220 biofilm formation. Thus, we argue that D-amino acids are not good *S. aureus* biofilm inhibitors.

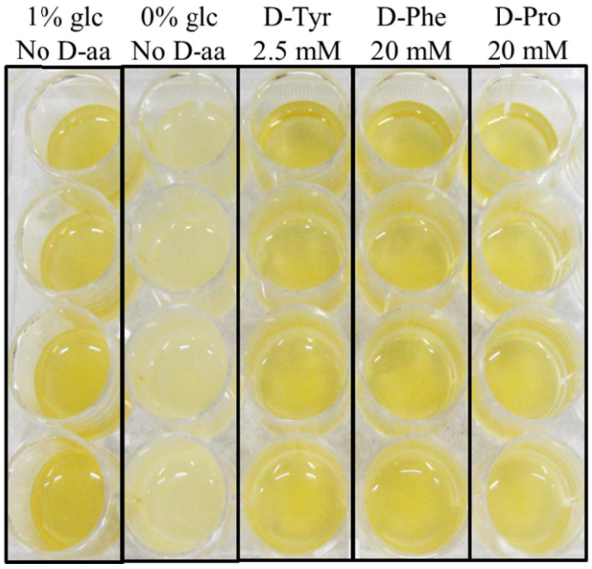

Figure 16. RN4220 biofilm D-amino acid inhibition experiment, before media removal. RN4220 *S. aureus* was grown for 24 hours in TSB with 0% or 1% glucose and additives, as listed on the figure.

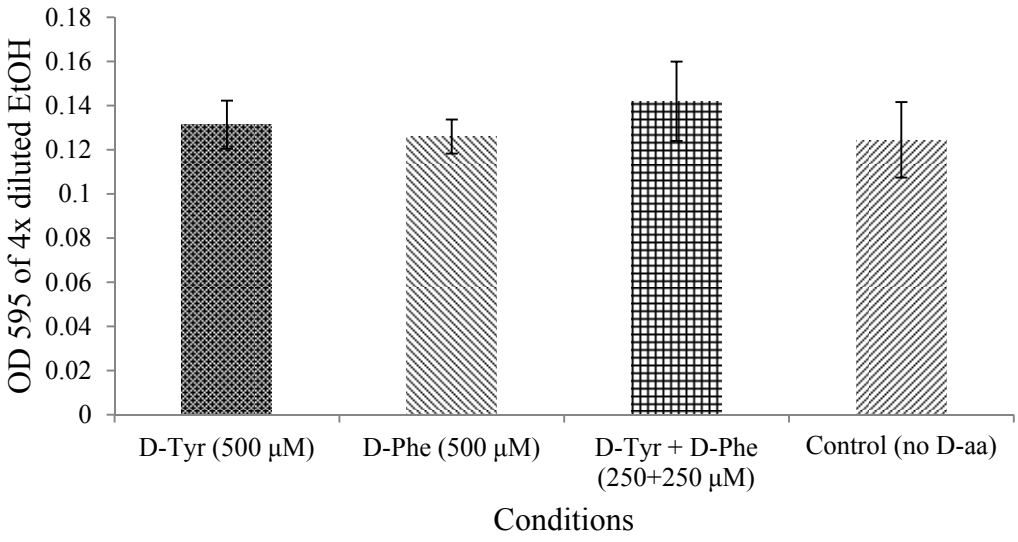

Figure 17. Chart representing the optical densities of diluted ethanol from the crystal violet assay of a D-amino acid RN4220 biofilm inhibition experiment. RN4220 was grown for 24 hours in TSB containing 1% glucose and additives, as listed on the figure. The error bars are based on the average sample standard deviation.

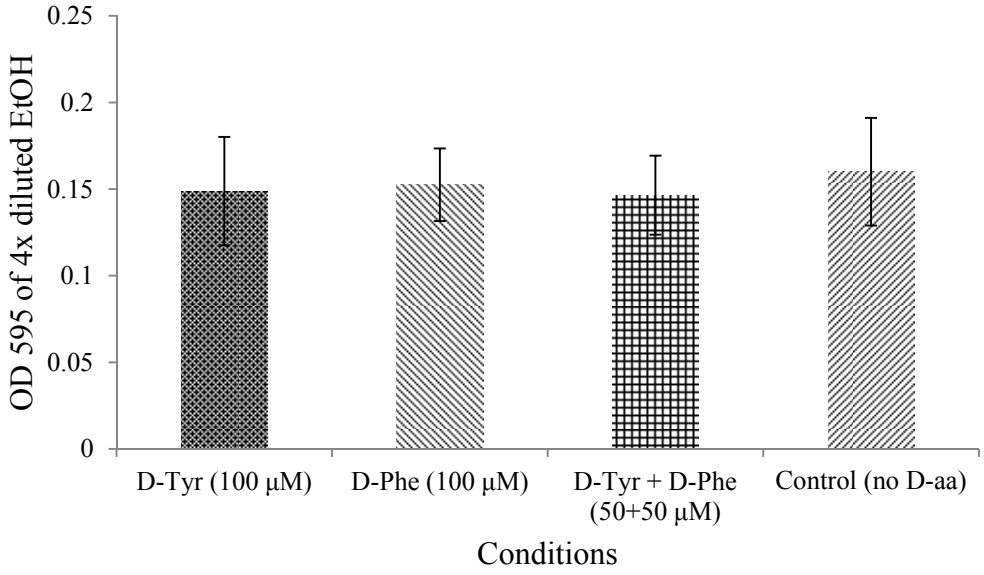

Figure 18. Chart representing the optical densities of diluted ethanol from the crystal violet assay of a D-amino acid RN4220 biofilm inhibition experiment. RN4220 was grown for 24 hours in TSB with 1% glucose and additives, as listed on the figure. The error bars are based on the average sample standard deviation.

Liquid Chromatography-Mass Spectrometry (LC-MS)

The samples analyzed with LC-MS were grown in glass test tubes, under the various conditions of 1) 1% glucose for 48 hours, 2) 1% glucose and 100 μM D-tyrosine for 48 hours, 3) no additives for 48 hours, and 4) 2.5 mM D-tyrosine for 24 hours. Samples from the conditions 1 and 2 formed biofilm. Samples from the conditions 3 and 4 did not form biofilm. The samples with biofilm were grown in 1% glucose, whereas the samples without biofilm were grown in the absence of glucose. These samples were analyzed with LC-MS to compare the peptidoglycan composition of samples grown without D-tyrosine to those grown with D-tyrosine. We were specifically looking for the incorporation of D-tyrosine into the mutanolysin-digested peptidoglycan fragments, via replacement of the terminal D-alanines in the peptidoglycan structure.

In order to decipher the data obtained from LC-MS, it was necessary to create a library of masses and their respective mass-to-charge ratios for which to search. The library of potential peptidoglycan species was constructed by drawing out the structures of monomers and polymers of peptidoglycan in ChemBioDraw. Mutanolysin, which was the enzyme used to digest the cell wall, cuts peptidoglycan at the β1-4 glycosidic linkage between N-acetylmuramic acid and N-acetylglucosamine. The various subunits included in the library were peptidoglycan fragments with cleaved β1-4 glycosidic linkages. The library included monomers, dimers, trimers, tetramers, and pentamers, with various acetylation patterns, cross-linking, and some replacements of D-alanine with D-tyrosine.

The first step in analyzing the LC-MS data was to identify peaks in the chromatograms which corresponded to peptidoglycan. This involved comparing the peptidoglycan library with noticeable peaks in the chromatogram. Most of the peaks in

the chromatogram were under 1500 m/z, but many of the peaks corresponded to masses larger than 1500 because of multiple charges. The charge of the species can be determined based on the m/z difference between isotopic peaks. For example, for singly charged species, the isotopic peaks are different by 1 m/z unit. For doubly-charged species, the isotopic peaks are separated by 1/2 m/z. For triply-charged species, the they are separated by 1/3 m/z. For quadruply-charged species, the isotopic peaks are separated by 1/4 m/z, and so forth.

While looking at the various high intensity peaks and comparing their values to the library, one peak at 833.0392 m/z, which corresponded to a triply-charged species, was of interest. This peak had a mass-to-charge ratio that matched that of a triply-protonated doubly-acetylated peptidoglycan dimer with a pentaglycyl bridge, within 0.0033 a.m.u. of the exact mass of 2496.0987 a.m.u.. Figure 19 depicts the structure of the doubly acetylated peptidoglycan dimer with a pentaglycyl bridge. This peak was present in all of the samples. Figure 20 corresponds to the selective ion chromatogram of the 833.0392 m/z peak for all 4 samples. The compound elutes from the LC column at approximately 17 minutes. Figure 21 depicts the combined spectra for these selective ion chromatograms over the time range of 16.5 to 17.8 minutes. Figure 21 shows that the isotopic peak 833.3668 m/z is the most prominent peak of the set of 833.0392 m/z peaks. Figure 22 provides an enlarged spectrum of the isotopic peak distribution of the 833.0392 m/z peak, for sample 1. We show the enlarged spectrum only for sample 1, since the isotopic peak distribution is identical among the spectra of the various samples.

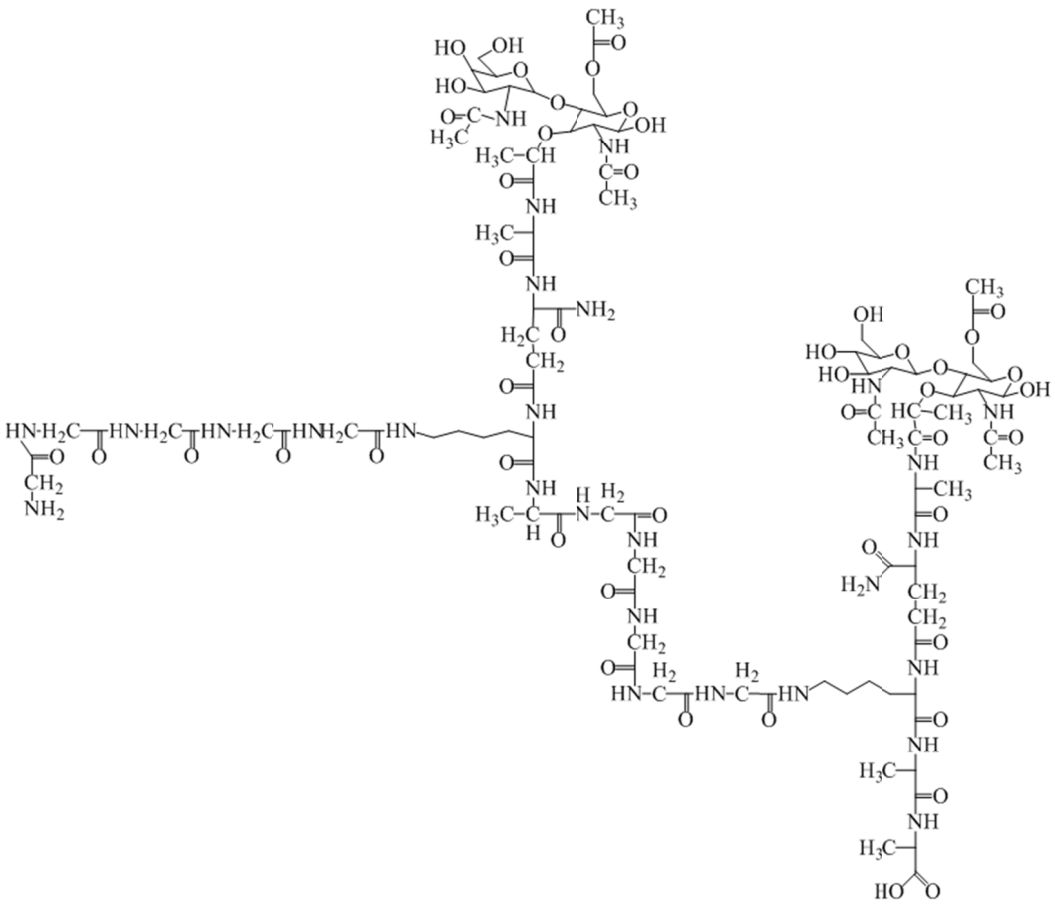

Figure 19. Chemical structure of doubly-acetylated peptidoglycan dimer, with each stem attached to a pentaglycyl bridge structure, and with a total molecular weight of 2497.4897 g/mol.

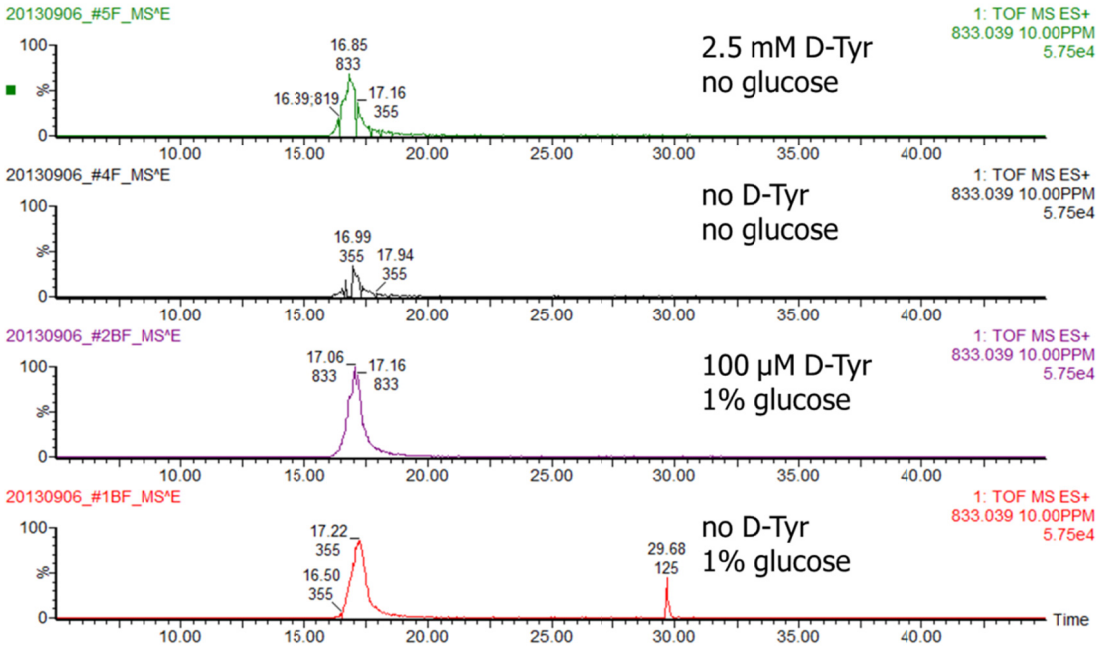

Figure 20. Selective ion chromatograms for 833.0392 m/z peak (doubly acetylated pentaglycine-peptidoglycan unit, Figure 19), within 10.00 ppm, for all four samples.

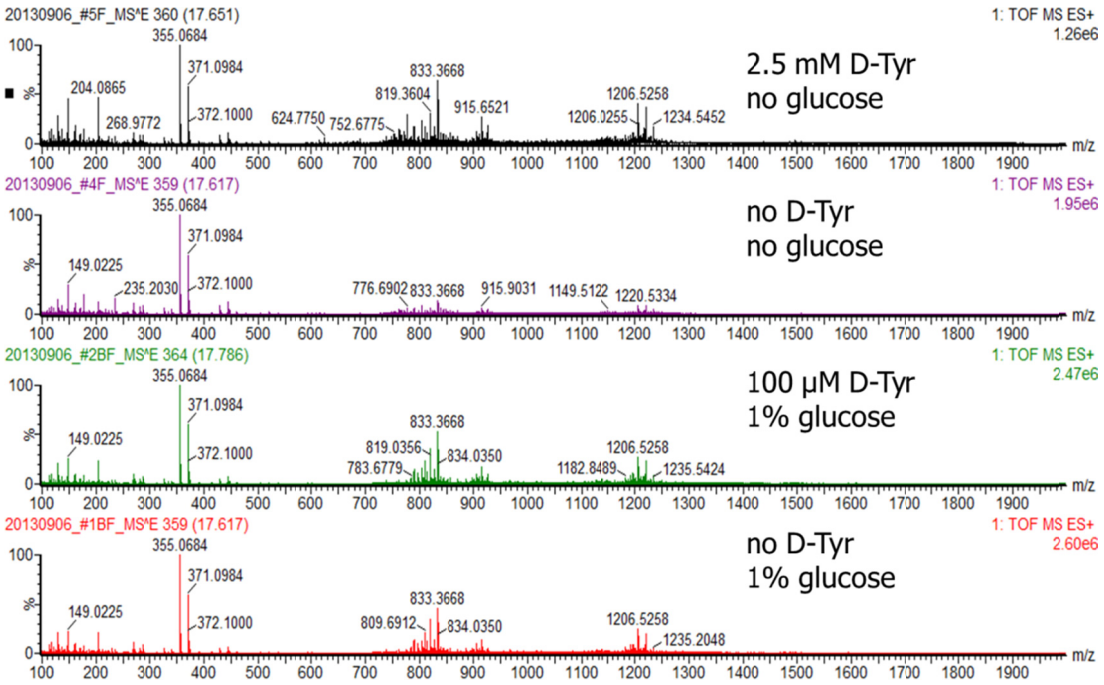

Figure 21. Accurate-mass spectra of mutanolysin-digested peptidoglycan from SA113 biofilm samples. The ionization current is plotted with respect to m/z (increases from left to right). The double acetylated peptidoglycan dimer with molecular weight of 2497.4897 is shown in the middle of the spectrum.

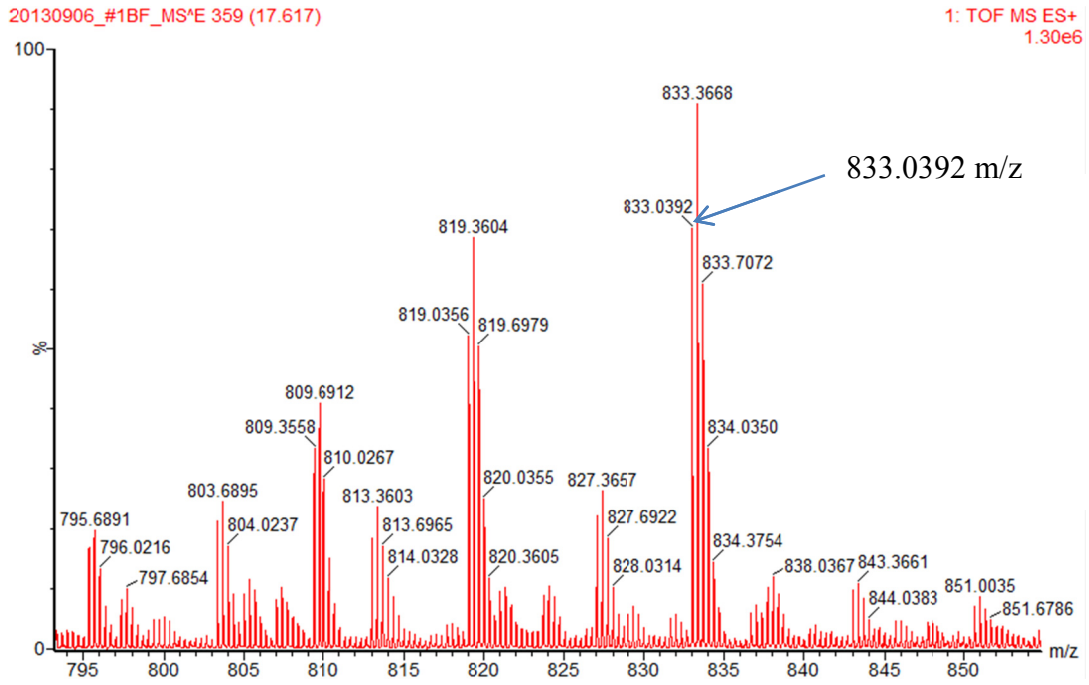

Figure 22. The enlarged spectrum of sample 1 from Figure 21, with visible isotopic peak distribution for 833.0392 m/z.

The second step, after searching for peaks corresponding to peptidoglycan fragments, was to look for peaks corresponding to peptidoglycan modified by the replacement of stem terminal D-alanines with D-tyrosine. None of the mass-to-charge ratios of the proposed peptidoglycan fragments containing D-tyrosine were found when searching through the samples. If D-tyrosine was incorporated in the fragments we thought might be present, it was in concentrations below the detection limit. Also, no noticeable peak differences are visible between the combined spectra of the samples grown with and without D-amino acids, as illustrated by Figures 23 and 24. Some differences are visible between the samples grown in the presence or absence of glucose in the growth media. Thus, the LC-MS analysis suggests that D-tyrosine was not significantly incorporated into the peptidoglycan structure.

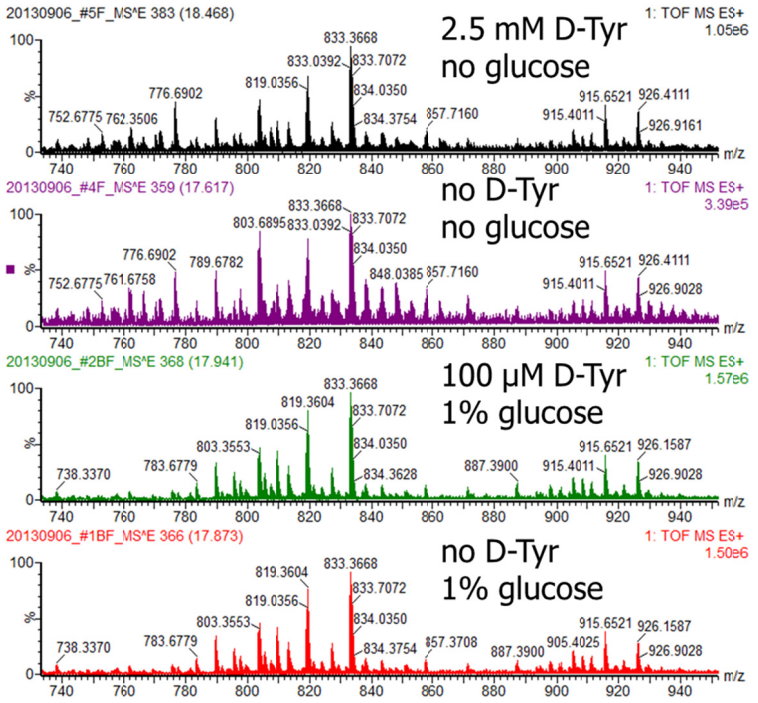

Figure 23. Enlarged combined accurate-mass spectra of mutanolysin-digested peptidoglycan from SA113 biofilm samples.

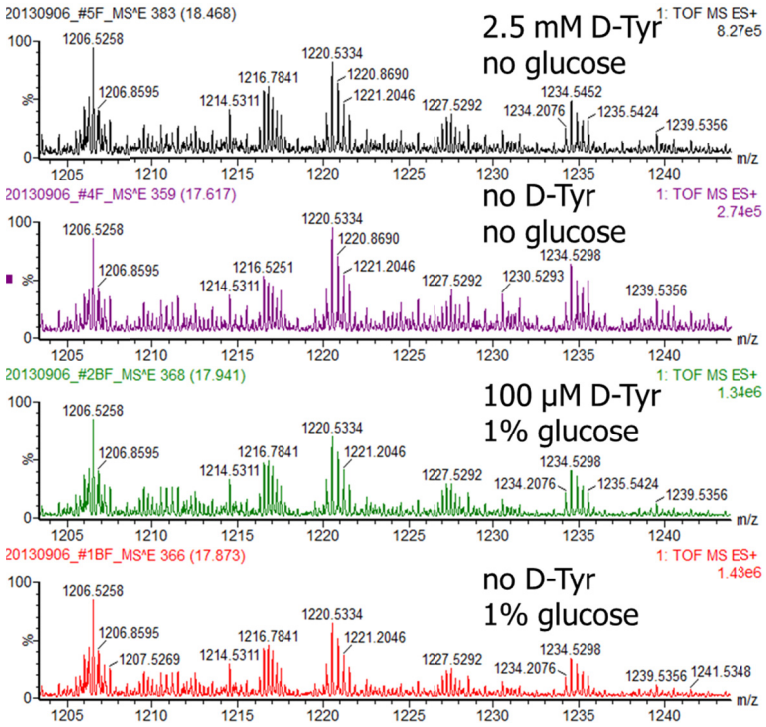

Figure 24. Enlarged combined exact-mass spectra of mutanolysin-digested peptidoglycan from SA113 biofilm samples.

CHAPTER FOUR

Discussion and Conclusions

Results from our observations, measurements of optical densities from crystal violet biofilm assays, and LC-MS analysis suggest that *S. aureus* (SA113 strain) biofilm is neither significantly dispersed nor inhibited by addition of D-phenylalanine, D-proline, or D-tyrosine to growth media. The lack of dispersion was surprising as dispersal was mentioned in the article initially reporting the effects of D-amino acids on biofilm growth (Kolodkin-Gal et al., 2010). The lack of significant biofilm inhibition was also surprising due to the reported inhibitive function of the D-amino acids that were used (Hochbaum et al., 2011). The lack of identifiable peptidoglycan fragments with D-tyrosine residues suggests that D-tyrosine does not inhibit biofilm formation by being incorporated into the peptidoglycan.

Biofilm Production

The presence of biofilm was identified based on certain characteristic features of biofilms. Biofilms are bacterial communities living within an adhesive matrix composed of polysaccharides, proteins, extracellular DNA and teichoic acids. The adhesive nature of biofilms is key. Biofilms are adhesive internally (forming a single pellet) and externally (adhering to surfaces). *Staphylococcal* biofilms often adhere to inert surfaces, such as indwelling medical devices. We determined that the *S. aureus* strain we grew, SA113, produced biofilm in the presence of glucose because the cells appeared to be attached to one another and the surfaces of 24-well plates. Biofilms are also usually

visualized by staining the cells with crystal violet. The crystal violet dye was another source of biofilm identification.

Our observations of biofilm growth show that SA113 is a strong biofilm-producing strain, in the presence of glucose. SA113 grown without glucose stayed primarily in the planktonic phase, suggesting that glucose plays a very important role in biofilm formation. The glucose may be a source of building material for the peptidoglycan, which we think plays a central role in biofilm formation. Our observations also suggest that SA113 biofilms adhere better to polystyrene surfaces than to glass. In fact, we had greater difficulty in retaining cells from washing away in the glass test tubes than in the plastic 24-well plates. Descriptions of the structure of SA113 biofilm provide examples of a particular biofilm phenotype, to which other biofilm phenotypes can be compared and contrasted. We observed biofilms that often formed web-like structures, with tick middle sections and attachments to the walls of each well. Characterization of biofilms is the first step toward increasing our understanding of biofilms. Future research should investigate the role that glucose plays in biofilm formation.

Errors in growing the biofilm are most likely quantitative errors. We assumed that a certain number of cells should produce the same amount of biofilm when placed under the same conditions. Differences in amounts of biofilm under identical conditions could be caused by statistical variation among the bacteria and by errors of the experimenter. Potential sources of human errors include misuse of the micropipette when preparing solutions, miscalibrated pipettes, and improper cleaning of glassware that could result in growth of other bacteria. Also, we noticed that significant evaporation (5-20%

of the volume in a well) sometimes occurred in outer wells. Parafilming the plates and placing them away from the hot air source in the incubator was used to correct for unequal drying. However, we observed when parafilming 24-well plates of some strains which normally produce biofilm, such as the lab strain RN4220, that those strains formed less biofilm. This could be explained by an understanding of the causes of biofilm growth. Biofilm growth in a lab strain may be triggered by adverse external factors, such as increasing concentrations of metabolic waste, due to a decrease in media volume because of drying. Thus, when the wells with RN4220 were parafilmed, the strain may not have sensed the need to form as much biofilm.

SA113 was chosen for these experiments because it is a clinically-isolated strain that produces large amounts of biofilm in the presence of glucose (Seidl et al., 2008). SA113 served as a model strain for biofilm studies. In one of our experiments, RN4220, which is a lab strain that produces less biofilm than SA113, was used. The measured optical densities for RN4220 biofilms exhibited results similar to those of SA113 biofilm crystal violet assays. In future biofilm studies, comparing the biofilm phenotypes of various strains could be useful. Branda et al.'s article suggests that "domesticated" bacterial strains can exhibit different growth patterns than natural isolates do (2001). Because of the medical relevance of microbial biofilm research, studying biofilm formation, dispersion, and inhibition using various laboratory and clinical strains is ideal.

The majority of our experiments were performed in 24-well plates. These plates are made of polystyrene. They are uncoated cell culture plates. These plates were chosen for *in vitro* analysis because Losick's group used similar polystyrene plates (Kolodkin-Gal et al., 2010, and Hochbaum et al., 2011) and the plates constitute a simple,

relatively inexpensive, and efficient method to study biofilm growth under various conditions. While our experiments did not focus on the surface on which the biofilm was grown, our initial comparison between biofilm grown in glass test tubes and in 24-well plates did raise some interesting questions about the interactions between various surfaces and biofilms. Catheters, a common surface on which *S. aureus* biofilms form, are often made of polyurethane, Teflon, silicones, polyethylene, polypropylene, polyvinyl chloride, polytetrafluoroethylene, and latex rubber (Treter, J.; Macedo, A. J., 2011 and Curtis, J.; Klykken, P., 2008). Also, formation of biofilms on indwelling medical devices can be affected by other components which can adsorb to surfaces (Ferrieres et al., 2007). Biofilms often contribute to chronic wounded infections, growing on biological tissues. Coraca-Huber et al. compared *S. aureus* biofilm growth on polystyrene plates with metal discs made of materials often used for orthopedic implants, suggesting a model for biofilm studies with different surfaces (2012). Additional types of inert surfaces, such as polystyrene, latex and silicone, or *in vivo* models should be used in biofilm studies. Such studies can more accurately depict the roles of bacterial biofilms in hosts and show how attachment surfaces and biofilms interact.

When the model of biofilm infection was originally developed, infections were thought of in terms of single-species (Wolcott et al., 2013). However, many biofilm infections are polymicrobial. This polymicrobial nature of biofilm may be a source of horizontal gene transfer, thus strengthening the biofilm communities. Perhaps cataloguing characteristics, such as morphology, of many types of biofilm could help establish connections between different biofilm structures, species, and external influences such as growth media and attachment surfaces. Current research into biofilm

morphology includes performing multi-resolution analysis of confocal laser scanning microscopy images (Yerly et al., 2008). Molecular methods must be used to identify and quantify various species present in polymicrobial biofilms. For example, PCR of the bacterial 16S rDNA gene (a genomic fingerprint) combined with mass spectrometry can be used (Wolcott et al., 2013). Sequencing techniques such as pyrosequencing (Dowd et al., 2008) or methods based on kinetic properties (Wolcott el al., 2013) can also be used. Future research should contribute to a library of biofilm morphologies and connections between bacterial species commonly associated in biofilms.

Biofilm Dispersion

The results from visual observations and crystal violet assays indicated that D-tyrosine, D-phenylalanine, and D-proline do not disperse SA113 biofilm within 24 hours. These results are disappointing because of the tremendous medical application that would have been achievable with positive results. Hochbaum et al. reported that an equimolar 10 mM mixture of D-tyrosine, D-phenylalanine, and D-proline caused SC01 biofilm disassembly (2011). However, a high 10 mM equimolar mixture of D-amino acids would most likely be lethal. One thing to note concerning the preparation of media containing D-amino acids was the poor solubility of D-tyrosine. D-tyrosine only has a solubility of 2.5 mM in water at 25 °C (Sigma-Aldrich). In TSB media, the solubility of D-tyrosine appeared to be even less because of our inability to prepare 2.5 mM D-tyrosine solutions in which the D-tyrosine was completely dissolved.

Potential sources of error include incomplete mass transfer when weighing out the D-amino acids, instrument drift of the balance, and unequal washing away of unattached cells in each well for the crystal violet assay. Also, the low solubility of the D-amino

acids, especially D-tyrosine, could lower the actual concentrations of amino acids relative to the calculated concentration, which could lead to less inhibition. Preparing larger volumes of D-amino acid stock solutions would have made it easier to weigh out the small amounts of amino acids required. More rigorous washing of a more robust biofilm produced by a different strain might make the crystal violet results more uniform.

The crystal violet assay is a common way to quantify biofilm growth. Crystal violet is usually used because it is an inexpensive and relatively simple colorimetric assay. Based on personal experience, some of the disadvantages of the assay include the fact that it is somewhat messy and mostly a qualitative quantitation approach. A crystal violet assay is a great way to detect traces of bacteria or to qualitatively compare amounts of biofilm. However, relative standard deviations ranging from 6 to 75% indicate the results have low precision. This low precision can be due to variation of biofilm growth between wells, but it could also be caused by an imprecise assay method. Increasing the number of samples could help reduce relative standard deviations. Using different assays and comparing the results with those from crystal violet assays could help validate the crystal violet method or point to additional sources of error.

Other techniques used to quantify biofilm growth include the determination of colony forming units (c.f.u.) after desorption, the use of high resolution microscopic techniques such as scanning electron microscopy, environmental scanning electron microscopy (SEM), transmission electron microscopy, cryo-electron microscopy, and atomic form microscopy, and the staining of cells with crystal violet, safranin or fluorescent dyes in combination with UV-Vis spectroscopy or ELISA (Hannig et al., 2010). Many sensitive techniques exist which can be used to more accurately quantify

biofilm growth than the crystal violet assay. However, many of these techniques are more expensive, labor-intensive and time-intensive. The traditional method for quantification by determination of the number of c.f.u. determines the number of active bacteria, but cannot be used to reliably quantify semi-planktonic bacteria, as may be present in biofilms (Hannig et al., 2010). The high resolution microscopy techniques present many challenges, such as sometimes requiring the samples to be coated, dehydrated, and under vacuum. The main problems with microscopy techniques are the extensive preparations necessary and the complexities of the techniques (Hannig et al., 2010). Three-dimensional microscopy visualization is useful for learning more about biofilm structure and morphology, but is more complex than needed to simply quantify biofilms.

Staining seems to be the overall best technique for experiments similar to ours. However, crystal violet assays used in combination with better detection methods may be more precise. Peeters et al. compared 6 different staining assays for quantifying biofilms of various species, such as *Pseudomonas aeruginosa* and *S. aureus*, in microtiter plates (2008). Their results showed high reproducibility and applicability for most isolates, with the exception of the use of the crystal violet assay for *P. aeruginosa* strains (Peeters et al., 2008). Also, the crystal violet and Syto9 assays did not allow differentiation between dead and alive cells (Peeters et al., 2008). Differences between Peeters et al.'s crystal violet assay and ours involved the use of different *S. aureus* strains, different ways of measuring absorbance (manually vs. with a plate reader), slight procedural variations such as using acetic acid instead of ethanol to release bound crystal violet, and the amount of runs (24 wells/experimental set-up vs. 3-6 wells/experimental set-up). The

crystal violet assay is a cheap and simple way to quantify biofilm, but its reliability should be verified for our experiments.

Finding compounds and techniques which can disrupt biofilms is very medically relevant because of the ineffectiveness of antibiotics against biofilm-producing species, especially in light of the increasing number of antibiotic-resistant bacteria. Our results showed that D-tyrosine, D-phenylalanine, and D-proline failed to disrupt SA113 biofilms. In current research, some proposed compounds and techniques to disrupt *S. aureus* biofilms include silk fibroin-silver nanoparticle composites (Fei et al., 2013), enzymes such as α-amylase (Kalpana et al., 2012), antibiotics like daptomycin (Roveta et al., 2008), and the use of lasers (Baffoni et al., 2012 and Krespi et al., 2011). Fei et al. used SEM and confocal laser scanning microscopy (CLSM) to observe the effects of silver nanoparticles on mature methicillin-resistant *S. aureus* (MRSA) (2013). Based on their descriptions and SEM and CLSM images, the biofilms began to break apart and more cells died with silver nanoparticle concentrations equal to or greater than the determined minimum bactericidal concentration (MBC). Silver nanoparticles are known to have antimicrobial properties, but the particles can be easily oxidized. Fei et al. present a method to stabilize silver nanoparticles.

Kalpan et al. used light microscopy to visualize the effects of α-amylase from a marine *B. subtilis* on mature biofilms (2012). Based on their observations, this enzyme can disrupt biofilms at its biofilm inhibitory concentration (BIC), determined with spectrophotometric assays and microscopic visualization (Kaplan et al., 2012). Roveta et al. did not describe in detail how the effects of daptomycin on biofilm disruption were tested, but did claim that daptomycin disrupted mature biofilm (2008). Their findings

suggest that more research is needed. Baffoni et al. showed that, unlike Krespi et al.'s results, near infrared laser irradiation of *S. aureus* and *P. aeruginosa* biofilms does not significantly disrupt biofilms (2012). However, Baffoni et al. suggested that combinatorial uses of lasers with antimicrobial therapy may be more effective. The best methods to kill biofilm-producing bacteria are to use combinatorial methods, which include antibiotics and other biofilm-disrupting tools such as silk fibroin-silver nanoparticles or lasers. Future research should examine the effects of combinatorial strategies on biofilm-producing strains *in vivo*.

Biofilm Inhibition

Our results indicated that concentrations ranging from 10 μM to 2.5 mM of D-tyrosine, D-phenylalanine, and D-proline do not inhibit SA113 biofilm growth. These results contradict those obtained by Kolodkin-Gal et al. (2010) and Hochbaum et al. (2011). In fact, we used concentrations of D-amino acids equal to and greater than those used in both papers, but obtained less noticeable changes in biofilm growth. Differences between our procedure and the procedure in Hochbaum et al.'s article include the use of different strains (SA113 vs. SC01) and different concentrations of media supplements (0% vs. 3% NaCl and 0.5% vs. 1% glucose). The most likely cause of difference between the results is the use of different strains. SA113 is a prolific biofilm former, probably because as a clinical isolate, it has been bred to form biofilm. The Losick group may have stumbled across a strain which is significantly affected by D-amino acids present in the growth media. Based on our results, D-amino acids are not universal biofilm inhibitors. These results point to the necessity in research of this nature to examine the effects of potential biofilm disruptors and inhibitors on a variety of strains.

Potential sources of error in the inhibition experiments most likely stem from errors made during preparation of D-amino acid solutions and during the crystal violet assay. Sources of error in D-amino acid preparation include instrument drift of the balance, incomplete mass transfer, and incomplete dissolution of the D-amino acids. Sources of error during the crystal violet assay include irregular washing between wells due to variation in the force of rinse added and removed, and incomplete rinsing and drying of cuvettes between optical density measurements. One should note that despite potential variation in the crystal violet assay, no remarkable decrease in SA113 biofilm growth was observed under D-amino acid conditions. Another source of error is uneven drying of wells in the incubator. To improve similar types of experiments, D-amino acid solution preparation could be improved with larger masses to be weighed. The crystal violet assay could be improved by using a plate reader and multichannel or electrical micropipettes. Parafilming the plates can help reduce error due to uneven drying. Increasing the number of replicate tests could help reduce relative standard deviation.

Biofilm inhibition is an important area of research, especially because of the increasing number of antibiotic-resistant strains. Current research in finding effective *Staphylococcus aureus* biofilm inhibitors has taken three routes. One area of research deals with biomaterial engineering, another concerns natural products chemistry, and a third deals with synthetic chemistry. Biomaterial engineering research focuses on the effects of the microtopography and composition of surface materials on biofilm growth. Chung et al. designed a surface microtopography based on shark skin which showed positive results for inhibiting *S. aureus* biofilm growth (2007). The shark skin-like surface prevented biofilm formation for a duration of time that was three times longer

than the pre-biofilm time on smooth surfaces (Chung et al., 2007). Depan and Misra obtained results indicating that approximately 93% less *S. aureus* cells adhere to silicone surfaces with incorporated nanophase titania than without titania (2014). In this area of research, natural products chemistry focuses on searching for compounds which may inhibit biofilm growth, especially molecules that block quorum sensing, such as furanones (Pereira et al., 2014). Quorum sensing is a way that bacteria communicate with each other, based on population density (Bhardwaj et al., 2013). Natural products chemistry looks at potential compounds that are used medicinally in various parts of the world (Hobby et al., 2012; Chaieb et al., 2011; and Quave et al., 2008), and isolated from various plant and animal origins (Wang et al, 2011; Jiang et al, 2011; and Bendaoud et al., 2011). The Losick group's research was similar to some other natural products research in the fact that the discovery of a potential broad-range biofilm inhibitor began with observations of biofilm inhibition in a particular species. However, the inhibition mechanism proposed by Hochbaum et al. was not related to quorum sensing inhibition, but rather to the incorporation of D-amino acids into the cell walls (2011). Also, synthetic chemists have attempted to create molecules which interfere with biofilm formation, such as the MBX compounds, proposed to inhibit *Staphylococcal* and *Enterococcal* biofilm growth (Opperman et al., 2009).

Future research on the effects of D-amino acids on biofilm growth should not be pursued. The results obtained were not promising enough to warrant continued work on this particular topic. Additionally, conversation with other microbiology labs working with various species and strains suggested that they obtained similar negative results. Kolodkin-Gal et al. published an article about norspermidine's potential as a biofilm

disassembly factor of *B. subtilis*, *E. coli*, and *S. aureus* (2012). However, because of the importance of these results, Hobley et al. reexamined the key findings and determined that "norspermidine is not a self-produced trigger for biofilm disassembly" (2014). This interaction lowers the credibility of Kolodkin-Gal et al.'s previous but similar work with D-amino acids, especially with respect to our negative results. Our results do not conclusively negate Kolodkin-Gal et al.'s research. Instead, the results provide cautionary advice against investing time, work, and money in studying the effects of D-amino acids on *S. aureus* biofilm growth. Nevertheless, future research should continue to investigate how biofilms form and can be inhibited.

As a philosophical aside, our results raise questions about how scientific work which produces negative results is and should be perceived. Is it more difficult to publish such results? If so, is that the correct approach? Do negative results require more evidence than positive results? Does it just depend on the nature of the claims made? Should all results require the same amount of evidence? Science claims to be self-correcting. For example, publishing is based on a peer-review system and collaborative work is encouraged. Collaborations with others, especially people from different backgrounds, can reduce biases and improve research quality. Gould's book *The Mismeasure of Man* describes how science is very much influenced by cultural norms. Gould's work looks at how cultural ranking of people affected scientific questions and conclusions. Gould's fascinating book points to the necessities of thinking about how science is often done and how to improve. Scientific communities, organizations, and seminars are essential for pushing science to be self-critical. Publishing negative results

ought to be encouraged just as much as publishing positive results, since both types can provide more insight into how the world works and how to do "good" science.

Liquid Chromatography-Mass Spectrometry

Results from our LC-MS analysis of biofilm samples indicated that none of the potential peptidoglycan structures containing D-tyrosine that we could think of were present in the D-tyrosine biofilm inhibition experiment samples. The first step to analyzing the LC-MS data was to identify which peptidoglycan components were present, after a mutanolysin digest. Mutanolysin is an N-acetylmuramidase that cuts peptidoglycan at the β1-4 glycosidic linkage between N-acetylmuramic acid and N-acetylglucosamine. One peak of interest was at 833.0392 m/z, which could correspond to a triply protonated ion of a peptidoglycan dimer with double acetylation and a 5-glycine bridge. The second step was to look through the library of potential peptidoglycan fragments with incorporated D-tyrosine. D-tyrosine could have been incorporated in place of the terminal D-alanine. No corresponding m/z were isolated. Thus, the LC-MS analysis suggests that D-tyrosine is not significantly incorporated into the peptidoglycan structure, and cannot therefore be a mechanism of biofilm inhibition.

Potential sources of error include incomplete digestion of the cell walls due to an insufficient amount of time or denatured mutanolysin, an unclean UPLC column, instrument drift, low signal-to-noise ratio for minute concentrations, and errors in peak identification. The LC-MS samples were mutanolysin-digested cellular pellets that were filtered through a 30 kDa filter. Thus, the LC-MS samples contained cellular components other than peptidoglycan subunits, such as proteins, nucleic acids, lipids,

carbohydrates, etc. These other components could display peaks with m/z values close to those of interest. These could be a source of error in peak identification.

The instrument we used combined the separation techniques of ultra-performance liquid chromatography (UPLC) with mass spectrometry. Different molecules have different retention times in the UPLC column. Mass spectrometry separates ions based on mass-to-charge ratios. A mass spectrometer has three main sections: an ion source, a mass analyzer, and a detector. The ionization technique we used was electrospray ionization (ESI), which uses a high energy field to ionize molecules. ESI causes very little to no fragmentation of ions. ESI is a more recent ionization method, which is especially useful for analyzing large biomolecules with mass spectrometry (Fenn et al., 1989). Another recent ionization technique for large biomolecules is matrix-assisted laser desorption/ionization (MALDI), which uses a laser beam to ionize molecules incorporated in a matrix (Karas and Hillenkamp, 1988).

The mass analyzer in our instrument was a time-of-flight (TOF) mass analyzer. In TOF mass spectrometry, ions separate in a drift tube because of differences in velocity due to variations in mass. Mass spectrometry is a highly specific technique, and is therefore a very powerful tool for detection purposes. MALDI-TOF has become a prominent technique in microbiology for bacterial identification. However, ESI sample preparation is much easier and simpler than MALDI sample preparation, which involves incorporating the sample into a matrix. Fast and simple bacterial identification is especially important in large polymicrobial communities, which can be very easily found in biofilm-promoting environments (Clark et al., 2013). Research into applying and overcoming certain limitations of mass spectrometry is needed.

The LC-MS analysis of peptidoglycan in search of incorporated D-tyrosine was performed for two purposes. One purpose was related to the proposed mechanism of D-amino acid biofilm inhibition, and the other dealt with increased scientific knowledge about peptidoglycan organization and its role in biofilm formation. Hochbaum et al. suggested that D-amino acids inhibit biofilm formation by being incorporated into peptidoglycan in place of D-alanine, and then disrupting cell surface-associated proteins (Hochbaum et al., 2011). Cava et al. showed that non-canonical D-amino acids can modify peptidoglycan by being incorporated into the peptidoglycan (2011). Some of the enzymes responsible for peptidoglycan biosynthesis, and mediating incorporation of D-amino acids, include penicillin-binding proteins (PBP) (Lam et al., 2009). PBP4 can add D-amino acids to peptidoglycan *in vitro* (Lupoli et al., 2011). Therefore, the proposed mechanism of inhibition was plausible.

Our results indicated that D-tyrosine was not incorporated into the peptidoglycan. These results however might be connected to the Losick group's later findings about the effects of D-amino acids on another organism, *B. subtilis*. Leiman et al. published an article showing that D-amino acids inhibit biofilm formation in a *B. subtilis* strain that has a mutation in the *dtd* gene which encodes D-tyrosyl-tRNA deacylase (2013). The mutation causes a lack of regulation of misincorporated D-amino acids. Thus, Leiman et al. proposed the misincorporation of D-amino acids into proteins as the mechanism of biofilm inhibition. This mutation was strain-specific. Perhaps a similar specific mutation could explain Kolodkin-Gal et al. and Hochbaum et al.'s results concerning D-amino acid inhibition of *S. aureus* biofilm.

The next step in this particular research is to perform LC-MS analysis of SA113 cell wall isolates, in order to confirm the peak identities. LC-MS analysis of cell wall isolates could also point to other important peaks present in peptidoglycan samples. Data from LC-MS analysis of cell wall isolates, using this particular instrument, would be very useful for future LC-MS analyses of *S. aureus* peptidoglycan. Future research should look at (1) identifying typical mass spectrometry peaks of peptidoglycan, (2) comparing peptidoglycan from various species to learn more about peptidoglycan structure, and (3) investigating changes in peptidoglycan composition under various growth conditions, including in environments which promote biofilm formation. Peptidoglycan, a component of the outer membranes of gram-positive and gram-negative bacteria, has been extensively studied. However, while the composition of peptidoglycan is known, the organization of bacterial cell walls and the interactions between peptidoglycan and extracellular and intracellular components still have areas to be explored.

Conclusions

D-amino acids do not inhibit biofilm formation by being incorporated into the peptidoglycan of SA113, a clinical strain. Crystal violet biofilm assays indicated that SA113 required glucose for biofilm formation, suggesting that glucose plays a central role in biofilm development. Crystal violet biofilm assays also indicated that D-tyrosine, D-phenylalanine, and D-proline did not disrupt mature biofilm or inhibit biofilm formation of SA113. LC-MS data analysis suggested that D-tyrosine does not replace terminal D-alanines in peptidoglycan. Future research should focus on investigating the roles that glucose and peptidoglycan play in biofilm formation across a wide range of strains.

BIBLIOGRAPHY

Archer, N. K.; Mazaitis, M. J.; Costerton, J. W.; Leid, J. G.; Powers, M. E.; Shirtliff, M. E. Staphylococcus Aureus Biofilms: Properties, Regulation, and Roles in Human Disease. *Virulence* **2011**, *2*, 445–459.

Bendaoud, M.; Vinogradov, E.; Balashova, N. V.; Kadouri, D. E.; Kachlany, S. C.; Kaplan, J. B. Broad-Spectrum Biofilm Inhibition by Kingella Kingae Exopolysaccharide. *J. Bacteriol.* **2011**, *193*, 3879–3886.

Bhardwaj, A. K.; Vinothkumar, K.; Rajpara, N. Bacterial Quorum Sensing Inhibitors: Attractive Alternatives for Control of Infectious Pathogens Showing Multiple Drug Resistance. *Recent. Pat. Antiinfect. Drug. Discov.* **2013**, *8*, 68–83.

Branda, S. S.; Gonzalez-Pastor, J. E.; Ben-Yehuda, S.; Losick, R.; Kolter, R. Fruiting Body Formation by Bacillus Subtilis. *PNAS* **2001**, *98*, 11621–11626.

Branda, S. S.; Chu, F.; Kearns, D. B.; Losick, R.; Kolter, R. A Major Protein Component of the Bacillus Subtilis Biofilm Matrix. *Mol. Microbiol.* **2006**, *59*, 1229–1238.

Cava, F.; de Pedro, M. A.; Lam, H.; Davis, B. M.; Waldor, M. K. Distinct Pathways for Modification of the Bacterial Cell Wall by Non-Canonical D-Amino Acids: Distinct Pathways for Cell Wall Remodelling. *EMBO J.* **2011**, *30*, 3442–3453.

Cava, F.; Lam, H.; Pedro, M. A.; Waldor, M. K. Emerging Knowledge of Regulatory Roles of D-Amino Acids in Bacteria. *Cell. Mol. Life Sci.* **2010**, *68*, 817–831.

Centers for Disease Control and Prevention (CDC) *Antibiotic Resistance Threats in the United States, 2013*. Atlanta, GA, 2013.

Chaieb, K.; Kouidhi, B.; Jrah, H.; Mahdouani, K.; Bakhrouf, A. Antibacterial Activity of Thymoquinone, an Active Principle of Nigella Sativa and Its Potency to Prevent Bacterial Biofilm Formation. *BMC Complement. Altern. Med.* **2011**, *11*, 29.

Chuard, C.; Lucet, J. C.; Rohner, P.; Herrmann, M.; Auckenthaler, R.; Waldvogel, F. A.; Lew, D. P. Resistance of Staphylococcus Aureus Recovered from Infected Foreign Body in Vivo to Killing by Antimicrobials. *J. Infect. Dis.* **1991**, *163*, 1369–1373.

Chung, K. K.; Schumacher, J. F.; Sampson, E. M.; Burne, R. A.; Antonelli, P. J.; Brennan, A. B. Impact of Engineered Surface Microtopography on Biofilm Formation of Staphylococcus Aureus. *Biointerphases* **2007**, *2*, 89.

Coraça-Huber, D. C.; Fille, M.; Hausdorfer, J.; Pfaller, K.; Nogler, M. Staphylococcus Aureus Biofilm Formation and Antibiotic Susceptibility Tests on Polystyrene and Metal Surfaces: Methods for Biofilm in Vitro Growth. *J. Appl. Microbiol.* **2012**, *112*, 1235–1243.

Cucarella, C.; Solano, C.; Valle, J.; Amorena, B.; Lasa, I.; Penades, J. R. Bap, a Staphylococcus Aureus Surface Protein Involved in Biofilm Formation. *J. Bacteriol.* **2001**, *183*, 2888–2896.

Curtis, J.; Klykken, P. *A Comparative Assessment of Three Common Catheter Materials*; 52-1116-01; Dow Corning Corporation: 2008.

Depan, D.; Misra, R. D. K. On the Determining Role of Network Structure Titania in Silicone against Bacterial Colonization: Mechanism and Disruption of Biofilm. *Mater. Sci. Eng. C Mater. Biol. Appl.* **2014**, *34*, 221–228.

Donlan, M. R., Biofilms and Device-Associated Infections. *Emerg. Infect. Dis.* [Online] **2001**, 7, 2 http://wwwnc.cdc.gov/eid/article/7/2/70-0277_article.htm (accessed Apr 3, 2014).

Dowd, S. E.; Wolcott, R. D.; Sun, Y.; McKeehan, T.; Smith, E.; Rhoads, D. Polymicrobial Nature of Chronic Diabetic Foot Ulcer Biofilm Infections Determined Using Bacterial Tag Encoded FLX Amplicon Pyrosequencing (bTEFAP). *PLoS ONE* **2008**, *3*, e3326.

Fei, X.; Jia, M.; Du, X.; Yang, Y.; Zhang, R.; Shao, Z.; Zhao, X.; Chen, X. Green Synthesis of Silk Fibroin-Silver Nanoparticle Composites with Effective Antibacterial and Biofilm-Disrupting Properties. *Biomacromolecules* **2013**, *14*, 4483–4488.

Fenn, J. B.; Mann, M.; Meng, C. K.; Wong, S. F.; Whitehouse, C. M. Electrospray Ionization for Mass Spectrometry of Large Biomolecules. *Science* **1989**, *246*, 64–71.

Ferrières, L.; Hancock, V.; Klemm, P. Specific Selection for Virulent Urinary Tract Infectious Escherichia Coli Strains during Catheter-Associated Biofilm Formation. *FEMS Immunol. Med. Microbiol.* **2007**, *51*, 212–219.

Geoghegan, J. A.; Corrigan, R. M.; Gruszka, D. T.; Speziale, P.; O'Gara, J. P.; Potts, J. R.; Foster, T. J. Role of Surface Protein SasG in Biofilm Formation by Staphylococcus Aureus. *J. Bacteriol.* **2010**, *192*, 5663–5673.

Goerke, C.; Wolz, C. Adaptation of Staphylococcus Aureus to the Cystic Fibrosis Lung. *Int. J. Med. Microbiol.* **2010**, *300*, 520–525.

Gould, S. J. *The Mismeasure of Man*; Norton & Complany, Inc: New York, 1996.

Hamilos, D. L. Host-Microbial Interactions in Patients with Chronic Rhinosinusitis. *J. Allergy Clin. Immunol.* **2013**, *131*, 1263–1264, 1264.e1–6.

Hannig, C.; Follo, M.; Hellwig, E.; Al-Ahmad, A. Visualization of Adherent Micro-Organisms Using Different Techniques. *J. Med. Microbiol.* **2010**, *59*, 1–7.

Herrmann, M.; Vaudaux, P. E.; Pittet, D.; Auckenthaler, R.; Lew, P. D.; Schumacher-Perdreau, F.; Peters, G.; Waldvogel, F. A. Fibronectin, Fibrinogen, and Laminin Act as Mediators of Adherence of Clinical Staphylococcal Isolates to Foreign Material. *J. Infect. Dis.* **1988**, *158*, 693–701.

Hobby, G. H.; Quave, C. L.; Nelson, K.; Compadre, C. M.; Beenken, K. E.; Smeltzer, M. S. Quercus Cerris Extracts Limit Staphylococcus Aureus Biofilm Formation. *J. Ethnopharmacol.* **2012**, *144*, 812–815.

Hobley, L.; Kim, S. H.; Maezato, Y.; Wyllie, S.; Fairlamb, A. H.; Stanley-Wall, N. R.; Michael, A. J. Norspermidine Is Not a Self-Produced Trigger for Biofilm Disassembly. *Cell* **2014**, *156*, 844–854.

Hochbaum, A. I.; Kolodkin-Gal, I.; Foulston, L.; Kolter, R.; Aizenberg, J.; Losick, R. Inhibitory Effects of D-Amino Acids on Staphylococcus Aureus Biofilm Development. *J. Bacteriol.* **2011**, *193*, 5616–5622.

Jiang, P.; Li, J.; Han, F.; Duan, G.; Lu, X.; Gu, Y.; Yu, W. Antibiofilm Activity of an Exopolysaccharide from Marine Bacterium Vibrio Sp. QY101. *PLoS ONE* **2011**, *6*, e18514.

Kalpana, B. J.; Aarthy, S.; Pandian, S. K. Antibiofilm Activity of A-Amylase from Bacillus Subtilis S8-18 Against Biofilm Forming Human Bacterial Pathogens. *Appl. Biochem. Biotechnol.* **2012**, *167*, 1778–1794.

Karas, M.; Hillenkamp, F. Laser Desorption Ionization of Proteins with Molecular Masses Exceeding 10,000 Daltons. *Anal. Chem.* **1988**, *60*, 2299–2301.

Karatan, E.; Watnick, P. Signals, Regulatory Networks, and Materials That Build and Break Bacterial Biofilms. *Microbiol. Mol. Biol. Rev.* **2009**, *73*, 310–347.

Keren, I.; Kaldalu, N.; Spoering, A.; Wang, Y.; Lewis, K. Persister Cells and Tolerance to Antimicrobials. *FEMS Microbiol. Lett.* **2004**, *230*, 13–18.

Kolodkin-Gal, I.; Romero, D.; Cao, S.; Clardy, J.; Kolter, R.; Losick, R. D-Amino Acids Trigger Biofilm Disassembly. *Science* **2010**, *328*, 627–629.

Krespi, Y. P.; Kizhner, V.; Nistico, L.; Hall-Stoodley, L.; Stoodley, P. Laser Disruption and Killing of Methicillin-Resistant Staphylococcus Aureus Biofilms. *American J.Otolaryngol.* **2011**, *32*, 198–202.

Kuru, E.; Hughes, H. V.; Brown, P. J.; Hall, E.; Tekkam, S.; Cava, F.; de Pedro, M. A.; Brun, Y. V.; VanNieuwenhze, M. S. In Situ Probing of Newly Synthesized Peptidoglycan in Live Bacteria with Fluorescent D-Amino Acids. *Angew. Chem. Int. Ed. Engl.* **2012**, *51*, 12519–12523.

Lam, H.; Oh, D.-C.; Cava, F.; Takacs, C. N.; Clardy, J.; de Pedro, M. A.; Waldor, M. K. D-Amino Acids Govern Stationary Phase Cell Wall Remodeling in Bacteria. *Science* **2009**, *325*, 1552–1555.

Losick, R.; Clardy, J.; Kolter, R.; Kolodkin-Gal, I.; Romero, D.; Cao, S. D-Amino Acids for Use in Treating Biofilms. Patent Application. WO 2011085326 A1, January 10, 2011.

Lupoli, T. J.; Tsukamoto, H.; Doud, E. H.; Wang, T.-S. A.; Walker, S.; Kahne, D. Transpeptidase-Mediated Incorporation of D-Amino Acids into Bacterial Peptidoglycan. *J. Am. Chem. Soc.* **2011**, *133*, 10748–10751.

O'Neill, E.; Pozzi, C.; Houston, P.; Humphreys, H.; Robinson, D. A.; Loughman, A.; Foster, T. J.; O'Gara, J. P. A Novel Staphylococcus Aureus Biofilm Phenotype Mediated by the Fibronectin-Binding Proteins, FnBPA and FnBPB. *J. Bacteriol.* **2008**, *190*, 3835–3850.

Opperman, T. J.; Kwasny, S. M.; Williams, J. D.; Khan, A. R.; Peet, N. P.; Moir, D. T.; Bowlin, T. L. Aryl Rhodanines Specifically Inhibit Staphylococcal and Enterococcal Biofilm Formation. *Antimicrob. Agents Chemother.* **2009**, *53*, 4357–4367.

O'Toole, G. A.; Kolter, R. Initiation of Biofilm Formation in Pseudomonas Fluorescens WCS365 Proceeds via Multiple, Convergent Signalling Pathways: A Genetic Analysis. *Mol. Microbiol.* **1998**, *28*, 449–461.

Otto, M. Staphylococcal Biofilms. In *Bacterial Biofilms*; Romeo, T., Ed.; Springer Berlin Heidelberg: Berlin, Heidelberg, 2008; Vol. 322, pp. 207–228.

Peeters, E.; Nelis, H. J.; Coenye, T. Comparison of Multiple Methods for Quantification of Microbial Biofilms Grown in Microtiter Plates. *J. Microbiol. Methods* **2008**, *72*, 157–165.

Pereira, U. A.; Barbosa, L. C. A.; Maltha, C. R. A.; Demuner, A. J.; Masood, M. A.; Pimenta, A. L. Γ-Alkylidene-Γ-Lactones and Isobutylpyrrol-2(5H)-Ones Analogues to Rubrolides as Inhibitors of Biofilm Formation by Gram-Positive and Gram-Negative Bacteria. *Bioorg. Med. Chem. Lett.* **2014**, *24*, 1052–1056.

Quave, C. L.; Plano, L. R. W.; Pantuso, T.; Bennett, B. C. Effects of Extracts from Italian Medicinal Plants on Planktonic Growth, Biofilm Formation and Adherence of Methicillin-Resistant Staphylococcus Aureus. *J. Ethnopharmacol.* **2008**, *118*, 418–428.

Romero, D.; Aguilar, C.; Losick, R.; Kolter, R. Amyloid Fibers Provide Structural Integrity to Bacillus Subtilis Biofilms. *PNAS* **2010**, *107*, 2230–2234.

Roveta, S.; Marchese, A.; Schito, G. C. Activity of Daptomycin on Biofilms Produced on a Plastic Support by Staphylococcus Spp. *Int. J. Antimicrob. Agents* **2008**, *31*, 321–328.

Sanchez, C. J.; Prieto, E. M.; Krueger, C. A.; Zienkiewicz, K. J.; Romano, D. R.; Ward, C. L.; Akers, K. S.; Guelcher, S. A.; Wenke, J. C. Effects of Local Delivery of D-Amino Acids from Biofilm-Dispersive Scaffolds on Infection in Contaminated Rat Segmental Defects. *Biomaterials* **2013**, *34*, 7533–7543.

Schroeder, K.; Jularic, M.; Horsburgh, S. M.; Hirschhausen, N.; Neumann, C.; Bertling, A.; Schulte, A.; Foster, S.; Kehrel, B. E.; Peters, G.; et al. Molecular Characterization of a Novel Staphylococcus Aureus Surface Protein (SasC) Involved in Cell Aggregation and Biofilm Accumulation. *PLoS ONE* **2009**, *4*, e7567.

Seidl, K.; Goerke, C.; Wolz, C.; Mack, D.; Berger-Bachi, B.; Bischoff, M. Staphylococcus Aureus CcpA Affects Biofilm Formation. *Infect. Immun.* **2008**, *76*, 2044–2050.

Sigma-Aldrich. L-Tyrosine Product Information. https://www.sigmaaldrich.com/content/dam/sigma-aldrich/docs/Sigma-Aldrich/Product_Information_Sheet/t3754pis.pdf (accessed Apr 3, 2014).

Swoboda, J. G.; Campbell, J.; Meredith, T. C.; Walker, S. Wall Teichoic Acid Function, Biosynthesis, and Inhibition. *Chembiochem* **2009**, *11*, 35–45.

Treter, J.; Macedo, A. J. Catheters: A Suitable Surface for Biofilm Formation. In *Science against microbial pathogens: communicating current research and technological advances*; Méndez-Vilas, A., Ed.; Formatex: Badajoz, Spain 2011; Vol. 2; pp. 835-842.

Vollmer, W.; Blanot, D.; de Pedro, M. A. Peptidoglycan Structure and Architecture. *FEMS Microbiol. Rev.* **2008**, *32*, 149–167.

Wang, D.; Jin, Q.; Xiang, H.; Wang, W.; Guo, N.; Zhang, K.; Tang, X.; Meng, R.; Feng, H.; Liu, L.; et al. Transcriptional and Functional Analysis of the Effects of

Magnolol: Inhibition of Autolysis and Biofilms in Staphylococcus Aureus. *PLoS ONE* **2011**, *6*, e26833.

Wolcott, R.; Costerton, J. W.; Raoult, D.; Cutler, S. J. The Polymicrobial Nature of Biofilm Infection: Polymicrobial Biofilm Infection. *Clin. Microbiol. Infect.* **2013**, *19*, 107–112.

Yerly, J.; Hu, Y.; Martinuzzi, R. J. Biofilm Structure Differentiation Based on Multi-Resolution Analysis. *Biofouling* **2008**, *24*, 323–337.